In Vivo Assessment of Leucine Stimulated Glucose Uptake in Brown Adipose Tissue

A thesis presented to

The Faculty of Graduate Studies

of

Lakehead University

by

BRENDA HUSKA

In partial fulfillment of requirements
for the degree of
Master of Science in Biology

January 17, 2017

Abstract

Activation of brown adipose tissue in mice, through the use of the amino acid leucine, was investigated. Brown adipose tissue has become a topic of interest in recent years, as activation of this tissue has been proposed as a potential target for obesity and type 2 diabetes treatment. This is because activation requires large amounts of energy, as well as circulating glucose, and stores of triglycerides. Previous work involving brown adipose tissue activation focuses on drugs with a known beta-adrenergic stimulus, which is one method of activation of brown adipose tissue, but few focus on potential dietary treatment. In order to assess activation due to leucine, ^{18}F-FDG uptake was measured using positron emission tomography after treatment with leucine. Using an analysis method of calculating standardized uptake value and maximum standardized uptake value, the level of ^{18}F-FDG uptake was quantified and used to judge activation. It was shown that leucine causes an additional increase to brown adipose tissue activation in a hyperglycaemic state. This finding opens the door for future research involving the method of action of leucine or testing if leucine treatment has the potential to treat hyperglycaemia.

Lay Summary

The following work was completed within the Department of Biology and thus adds to the the understanding of biology and fits with the department mission statement, “Faculty and students in the Department of Biology are bound together by a common interest in explaining the diversity of life, the fit between form and function, and the distribution and abundance of organisms”. It may not be immediately clear the fit of the following research to this mission statement, but the work allows for a better understanding of the underlying biological mechanisms that are at play in relation to the physical form of a mouse. Through research involving the internal bodily component called brown adipose tissue, a better understanding of the function of the tissue in the mouse is found. The research completed was to determine if treatment with the amino acid leucine can increase glucose uptake in brown adipose tissue, which would indicate that the tissue is active. Activity of this tissue is linked with an increase in energy expenditure, use of sugar from the blood stream, and stored fat use. It is thought that through activation of brown adipose tissue, hyperglycaemia, which is common in obesity and diabetes, can be treated or prevented. This knowledge on brown adipose tissue function could also allow for a translational link between mice and humans and relate these two very diverse species through this tissue, giving a better understanding of the function of the human brown adipose tissue.

Acknowledgements

I would like to thank first of all my co-supervisor and mentor, Dr. Lees. Without him I can confidently say that I would never have completed my degree, his understanding, compassion, and helpfulness are truly the reason I am completing this degree and this chapter of my life. Continued support on lab procedures, advice when things did not go as expected during PET imaging, and guidance on where to go next and what to know were incredibly helpful and appreciated. I would also like to thank my other co-supervisor Dr. Phenix. Your positive commentary, constructive ideas, patience, and friendliness helped me through many things during the early part of my degree. Although you were no longer close in distance, you always could be called on when I needed it and I appreciate all you have done for me in this journey. To my remaining committee member Dr. Schraft, I would like to thank you for your patience and input during this process. Your questions and point of view were always very helpful, and I appreciate all the time you put into this.

Next, I would like to thank Sarah Niccoli for her help with everything I did as well as her friendship and support. You helped me through many problems in the lab and were essential to imaging days. Your knowledge and assistance was key to experience and I can honestly say the Lees group would fall apart without you.

To Paige Ferrazzo, my fellow masters companion I would like to thank you for your help with my experiments, even when you had much better things to do, as

well as being there to navigate this experience together, reassure each other when things were tough, and your constant positive attitude and support, I couldn't be happier that we ended up in the same group.

I would also like to thank all my fellow NOSM students and companions for making the lab a lot more fun, and making it feel more like family than co-workers.

To my friends and family, thank you for putting up with me during this experience, your patience when I was busy or unable to come visit is appreciated so much, and I look forward to seeing a lot more of you all.

Lastly, I would like to thank my husband Dylan Carabott. You were there for me through everything, even crazily planning a wedding right in the middle of all this. You stopped me from completely going crazy and kept me together when I thought I couldn't make it. You watched all my presentations, helped me with my grammar, made sure I ate, and kept the house and animals in order when I was busy. Anything you could do to make my life easier, you did, and I don't know if you'll really know how much it meant to me. I'm excited to move on from school and into the next chapter with you. Thank you.

Table of Contents

1. Introduction:

With approximately 2 million Canadians suffering from type two diabetes (T2D) and 37% of Canadians being overweight, 24.5% of those being obese, there is a growing need for additional treatment and therapies to address this disease and health concerns [1], [2]. One growing area of interest to address this need is with brown adipose tissue (BAT). BAT has been known to be prevalent in small animals and infants. Due to advancements in imaging technology, recent studies have shown the presence of BAT in adult humans. As seen in Figure 1, depots are symmetrically located at the cervical-supraclavicular, paravertebral, mediastinal, and periadrenal regions [3]–[8].

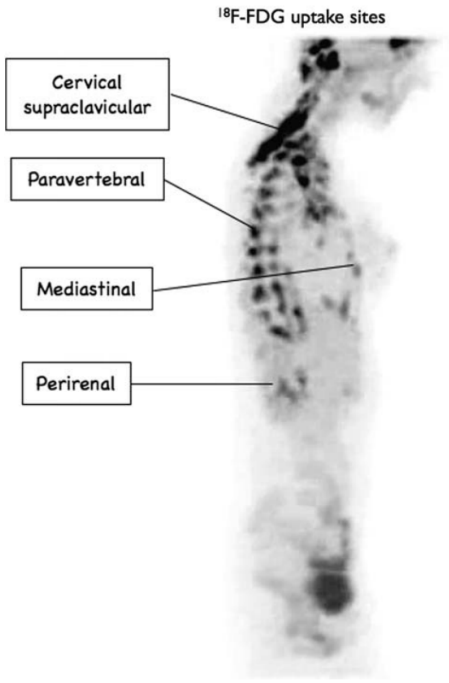

Figure 1: Fused positron emission tomography (PET)/computed tomography (CT) images showing ^{18}F-FDG uptake in human cervical-supraclavicular, paracertebral, mediastinal, and periadrenal regions that have been confirmed to be BAT depots [8]. Taken from D. Richard, et al., 2010.

With the discovery of BAT in adult humans interest in its function has peeked. BAT is known to be responsible for non-shivering thermogenesis as well as acting as an endocrine organ [9]. These properties make it ideal for increasing energy expenditure of the body and reducing the amount of glucose and fats in the blood stream, which can be useful when being applied to diabetic and overweight individuals [10]–[13].

Insulin is a hormone normally secreted from the β-cells of the pancreas, primarily in response to a meal or glucose intake. β-cells, that are clustered in islets, sense changes in plasma glucose levels and release insulin from secretary granules. The β-cells also respond to other nutrients in the blood stream such as monosaccharides, amino acids, and fatty acids, but to a lesser extent. Once released, insulin binds to insulin receptors located at various locations, which causes the use or storage of glucose within the body. In individuals with type 1 diabetes (T1D) and T2D, pancreatic β-cell dysfunction is an important factor to the disease pathogenesis. In T1D the mass and insulin secretary function of β-cells is decreased; the cause of this is linked to autoimmunity. The immunological activity, primarily through T lymphocytes, within the pancreas causes the destruction of β-cells. Conversely, chronic insulin resistance and loss of β-cell mass and function result in T2D; the primary cause of this is chronic hyperglycaemia, which is linked to obesity. Obesity is associated with impairment in energy metabolism, leading to increased intracellular fat content in skeletal muscle, liver, fat, and pancreatic islets. This chronic insulin resistance will

progress to T2D when the β-cells can no longer secrete necessary amounts of insulin to compensate for decreased insulin sensitivity and chronic hyperglycaemia. Hyperglycaemia is the constant entry of glucose into β-cells, which leads to insensitivity to glucose stimulation. This leads to the exhaustion of β-cell stores of insulin [14]. Eventually this leads to glucotoxicity and irreversible damage, leading to apoptosis of the β-cells. Chronic exposure of the β-cell to glucose and fatty acids is thought to be the cause of hyperglycaemia.

The diminished insulin response is often discussed in terms of stimulation from glucose, mainly caused after ingestion of a meal, but as mentioned previously, other nutrients have been shown to stimulate insulin release. Some amino acids have been shown to have this ability, often through enhancement of glucose stimulation, but also through adenosine triphosphate (ATP) production, and incretin-dependent pathways. Amino acids are organic compounds that contain an amine group as well as a carboxyl group, along with varying side chains, and make up the basis of many tissues within the body. Amino acids play important roles in biological functions and can be classified into various categories based on structure, properties, or relation to diet and activity. In terms of diet the classes of amino acids are essential, non-essential, and conditional. Essential amino acids are ones that are required by the body, but cannot be produced and instead must be supplied through diet. Non-essential amino acids can be produced within the body, either through the breakdown of proteins or from essential amino acids. Conditional amino acids are only required in times of

stress or illness. Of these categories, further properties can be subcategorized. Not all amino acids have the same effect on insulin release, some do not seem to elicit a response, such as isoleucine and valine as examples. Others, such as glutamic acid have a negative effect on insulin release. Lastly, as mentioned previously some amino acids produce an increase in insulin release; examples of these include glycine, leucine, serine, and alanine [15]. Leucine specifically has been shown to have the greatest effect out of these. Due to these responses it has been suggested that amino acids could play a role in diet recommendations for individuals with T2D or other insulin related diseases.

To look at the prospect of treatment with amino acids further, leucine has been investigated and is a main component of the proposed study. Leucine is a branched chain essential amino acid, that has been of interest originally for muscle protein synthesis purposes, due to it's ability to increase this process as well as increase muscle protein synthesis sensitivity to insulin [16]-[19]. As well as increasing protein synthesis, leucine has been shown to increase glucose uptake in skeletal muscle [20], [21]. The effect of leucine on glucose uptake in other tissues has not been investigated to the same extent as skeletal muscle, but it has been shown to improve glucose metabolism and reduce diet induced obesity. There is some evidence that this may partially be due to effects on BAT [21]. It is also known that leucine increases insulin release, which could partially explain the response of BAT due to it being an insulin sensitive tissue. The method of action of leucine in BAT has not been fully elucidated, the role of

insulin sensitivity as well as other potential pathways must be investigated further.

Promoting insulin sensitivity in BAT could be beneficial to metabolic expenditure as well as non-shivering thermogenesis. This is due to the fact that insulin resistance in BAT could have adverse effects on metabolic expenditure as well as non-shivering thermogenesis since it has been shown to limit β-adrenergic activity and reduces glucose uptake. Improving insulin sensitivity should improve β-adrenergic activity and in turn increase glucose uptake. Glucose uptake in BAT has been overlooked in the past, but recently its importance has become apparent, being it indicates activity within the tissue [22], [23]. This activity can be caused by either non-shivering thermogenesis or diet induced thermogenesis. Both of which are important for reducing glucose and fatty acid levels from the blood stream, as well as increasing metabolic expenditure. Developing strategies to stimulate BAT metabolism as well as understanding its function through diagnostic imaging could be an important tool in managing insulin resistance.

Literature indicates that an increase in BAT volume and BAT activity can improve glucose tolerance and insulin sensitivity in mice. One such tested this through transplantation of BAT in mice. The mice receiving the transplant had an increase in glucose tolerance, and compared to sham operated control mice, did not see a decrease in insulin sensitivity over time. These mice also saw a decrease in weight, fat mass. It was then tested if the transplantation could affect mice who

were fed a high-fat diet before and after BAT transplant from a chow-fed mouse. It was found that mice who received BAT transplant were able to avoid insulin resistance [24]. Other studies have indicated increasing BAT activation has had similar results in weight loss, fat mass, and insulin resistance [23], [25]-[27]. These results indicate BAT related therapies could be used as a treatment for insulin resistance, obesity, and in turn T2D; furthering the importance of understanding BAT function and stimulation via diagnostic imaging.

1.1. Research Question

To deal with the increasing and prominent issues associated with obesity and T2D, activating BAT is offered as a solution. Can leucine be used in a safe and effective way to activate BAT and which treatment creates the greatest effect? Can these treatments activate BAT without initial cold activation? What signalling pathway in BAT is being activated in response to leucine?

1.2 Specific Aims

1. To determine if glucose treatment can increase glucose uptake in BAT.

   Rationale: Glucose's ability, when given with 2-deoxy-2-(18F)fluoro-D-glucose (^{18}F-FDG), to cause an increased insulin release, leading to an increased glucose uptake in BAT will be determined using positron emission

tomography (PET). It is known that an increase in glucose levels stimulates insulin release in healthy individuals, causing normal glucose disposal. BAT has been shown to be an insulin responsive tissue, as well as diet responsive; the level of insulin release caused by the given glucose and the ability of this released insulin to in turn cause BAT to uptake glucose should be determined.

Hypothesis: With mice fasted for 5 hours prior to experiments, plasma glucose levels will be stable prior to glucose injection. It is hypothesized that the addition of glucose will increase BAT glucose uptake, due to the insulin responsive nature of BAT [28]-[31].

2. To determine if leucine alone or in the presence of glucose can increase glucose uptake in BAT.

Rationale: Leucine is a branched chain essential amino acid that has strong links with muscle protein synthesis along with insulin sensitivity [32]. Leucine has been shown to cause the greatest insulin release, upon infusion, compared to other amino acids. It also has little effect on plasma glucagon levels, only suppressing it slightly. It has been suggested that, due to these characteristics it can enhance glucose utilization in peripheral tissues [33]. Studies related to muscle protein synthesis and glucose uptake in muscle after an infusion of leucine, have shown that leucine does not increase

muscle protein synthesis unless also in the presence of glucose. This suggests that leucine increases the sensitivity of the tissue to insulin [16], [34]. Therefore, I propose to test the effect of leucine alone, and in combination with glucose, on glucose uptake in BAT.

Hypothesis: Based on the previously published data on effect of leucine and glucose on muscle protein synthesis, it is hypothesized that the leucine in combination with glucose will increase the glucose uptake of BAT, and not leucine alone.

3. To determine if glutamic acid in conjunction with glucose can increase uptake in BAT.

Rationale: Glutamic acid is a non-essential amino acid. It has been shown to produce no positive effects on insulin or glucagon production in vivo, unlike some other amino acids [33]. Some amino acids, such as leucine, serine, alanine, and glycine, for example, cause significant changes in insulin levels after infusion, and/or glucagon production. These amino acids cause an increase in both insulin and glucagon levels, with the exception of leucine, which only increases insulin levels, but not glucagon. Glutamic acid, however, does not cause any significant changes in either of these levels [33]. It will be used as an amino acid and glucose combination that will produce no uptake in order to compare with positive uptake results.

Hypothesis: It is hypothesized that there will be no increase in glucose uptake in BAT in response to the treatment of glutamic acid and glucose.

4. To determine the roles of insulin and β-adrenergic signalling targets in the stimulation of glucose uptake.

Rationale: Using known targets of both the insulin stimulated signalling pathway as well as the β-adrenergic signalling pathway will help determine the method of action of the treatments. Phosphorylated protein kinase B (p-Akt) will be used as an insulin stimulated signalling pathway target. During insulin stimulation insulin receptor substrate 1 (IRS-1) is phosphorylated at one of its tyrosine phosphorylation sites, allowing the docking of phosphatidylinositol 3-kinase (PI3K). This in turn leads to a signalling cascade that results in protein kinase B (Akt) phosphorylation. For a β-adrenergic stimulated signalling target, glycogen synthase kinase 3β (GSK-3β) will be used. This is a target of both insulin stimulated signalling as well as β-adrenergic signalling, however using information of both p-Akt and GSK-3β signalling conclusions about which pathway is active can be suggested.

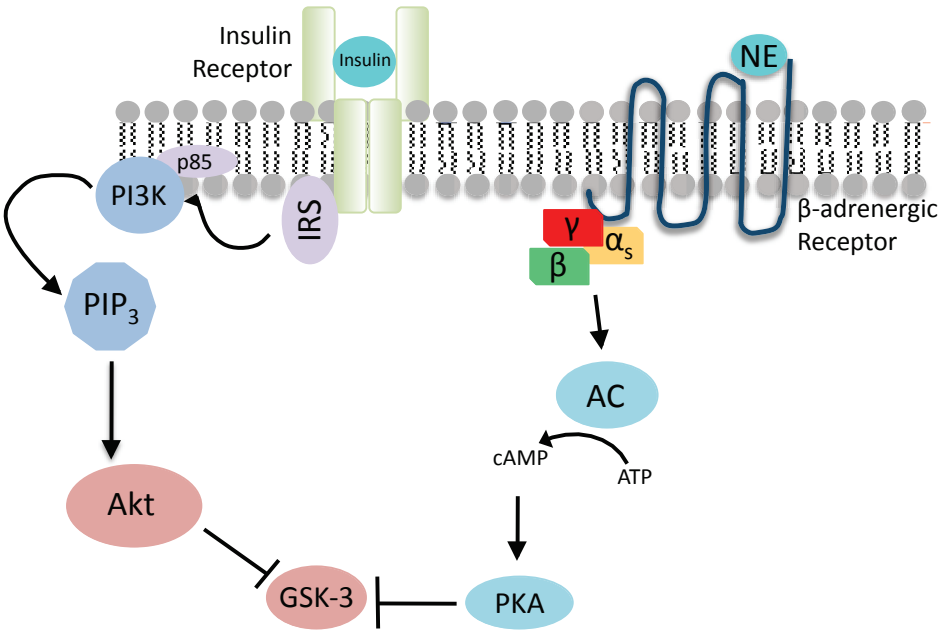

Figure 2: Signalling pathway due to insulin receptor activation and norepinephrine (NE) stimulation through the β-adrenergic receptor. The insulin receptor auto-phosphorylates causing insulin receptor subunits (IRS) to phosphorylate, leading to downstream Akt phosphorylation and inhibition of GSK-3β phosphorylation. The β-adrenergic receptor leads to the production of cAMP leading to eventual inhibition of GSK-3β.

Hypothesis: It is hypothesized that the combination of leucine and glucose will will activate both the insulin and β-adrenergic signalling pathways. Through the adrenergic pathway due to cold activation to produce thermogenesis, but will also activate through an insulin responsive pathway shown through phosphorylated AKT levels [35]–[38].

5. To determine if inhibition of the β-adrenergic receptors will diminish BAT uptake *in vivo*.

   Rational: Activation of BAT for non-shivering thermogenesis has been shown to occur through sympathetic activation of the β_3 adrenoceptor. This activation causes the increase in cyclic adenosine monophosphate (cAMP) levels, which in turn cause the activation of protein kinase A (PKA), leading to thermogenesis, refer to Figures 2 and 7. Literature suggests that diet-induced thermogenesis occurs through an insulin sensitive pathway, so by blocking nervous system and norepinephrine stimulation this pathway should still remain [22], [23], [39], [40]. If the measured BAT glucose uptake is lowered below a readable level using a beta-blocker, all activation is occurring through a β_3 mediated pathway and not an insulin sensitive pathway. If there is measured BAT glucose uptake remaining, activation is also occurring through a different pathway, likely insulin sensitive, and is likely due to the given treatments and not cold activation.

   Hypothesis: It is hypothesized that some BAT uptake will remain after inhibition.

1.3 Study Purpose

The purpose of the proposed study is to evaluate and further understand the mechanisms of glucose uptake specific to the tissues of interest. The ability to assess BAT activation using PET, through the level of glucose uptake in

response to various treatments and conditions will be determined. This will lead to whether leucine alone, or the presence of a hyperglycaemic conditions, can stimulate a BAT response. It will be assessed, whether these treatments have an effect on glucose uptake in other prominent tissues in the body. The aim of these studies is to provide insight into treatments that could be promising to be utilized to help treat obese or diabetic patients as a long-term treatment or in tandem with other medications and treatments. If promising candidates are identified, more research into the method of action and potential therapeutic use could be investigated by future researchers.

2. Literature Review

2.1 Positron Emission Tomography

PET is a medical imaging modality that makes use of a radiotracer to image internal processes of the body. A radiotracer is a chemical compound that has a radioactive positron emitting isotope attached. This radiotracer is injected into the body where it generally mimics the non-radioactive form of the same compound. The radiotracer travels through the body following the metabolic pathway of the compound, until reaching the final destination or until the altered chemical makeup does not allow further metabolic processing. As the tracer travels and once it reaches the desired destination, positrons and neutrinos are emitted from the radioactive isotope as they spontaneously decay, refer to Figure 3 [41], [42].

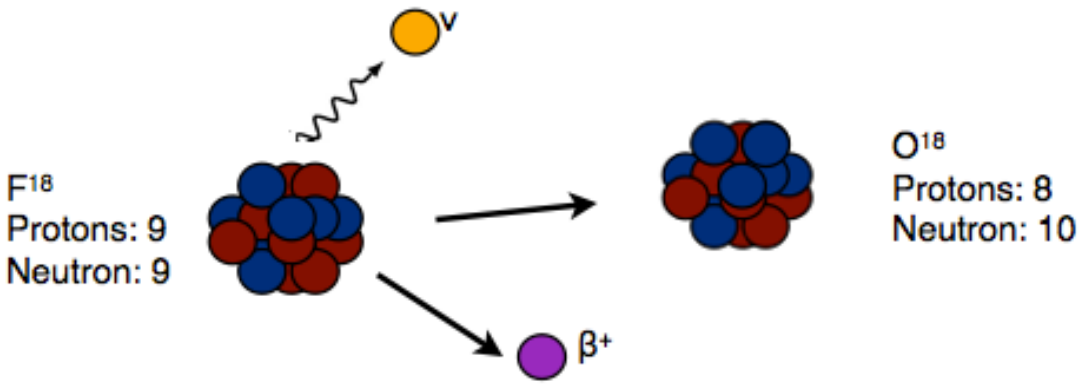

Figure 3: An illustration of fluorine 18 spontaneously decaying to oxygen 18. A proton from the fluorine 18 nucleus decays to a neutron. The products of this decay are a β+ particle known as a positron and a neutrino.

This positron travels a small distance, depending on positron energy, where it will reach an electron present within the body. A positron emitted from a decaying fluorine-18 atom has a maximum energy of 0.635MeV, corresponding to a maximum range of 2.4mm and a mean range of 0.6mm [42]-[44]. These distances are what determine the maximum resolution that can be achieved with PET, since where the positron is emitted, to where it travels will differ by the range it can travel. At this point there is an annihilation of the positron and electron, where coincident gamma rays, with an energy of 511keV, are released. These gamma rays are emitted 180° from each other and at the same time. Detectors located in either a ring or panel set around the subject detect these gamma rays. The detectors rely on coincidence electronics and analysis to determine the origin of the gamma rays detected. A line of response is created from the location of detection of a pair of gamma rays. The line of response leads

to the location of the initial annihilation event [41], [42]. A visual of the line of response and determination of coincidence can be seen in Figure 4.

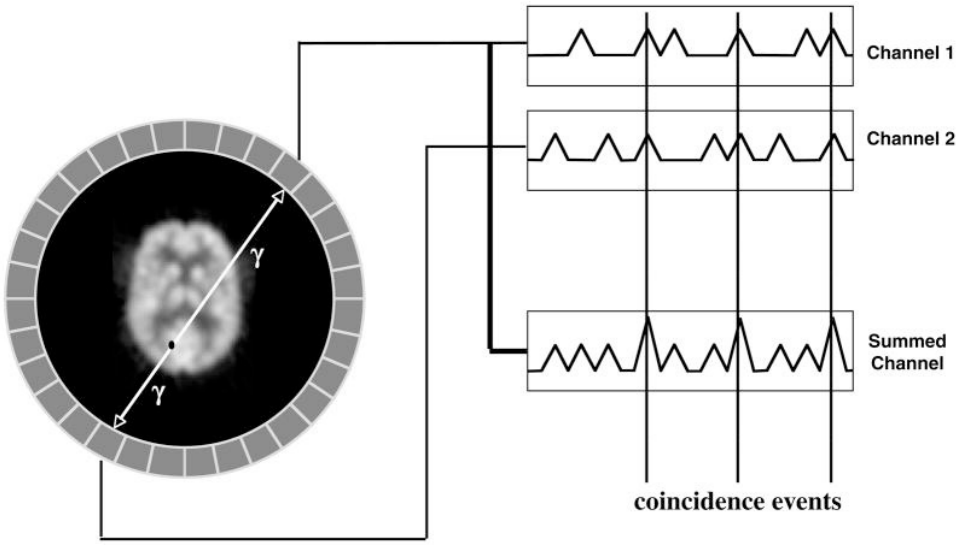

Figure 4: Typical PET system geometry. The object being scanned is usually surrounded by rings of detectors. Each detector acts as a single event detector (records single gamma-ray events). When single events occur within a short time of each other, they are considered in coincidence and saved as a prompt event. The time difference to be considered in coincidence is usually a few nanoseconds [45]. Taken from T. K. Lewellen, 2008.

2.1.1 Limiting Factors

In an ideal situation the detected gamma rays are perfectly coincident, but in practice there are some anomalies that affect image quality. The emitted gamma rays can be scattered, which causes one or both to leave the line of response. Though a scattered event is a true coincidence event, because the line of response will be off, the spatial resolution and image contrast will be diminished.

There can also be accidental coincidence that happens at random. In this case two positrons annihilate, creating a gamma ray from each of the annihilations. Examples scattering and random coincidence are shown in Figure 5. If these two events occur close enough together, the electronics will link the two events as a true coincidence event. Since this last form of coincidence occurs randomly, there will be an even distribution throughout the detection time and many will be excluded by imposing a coincidence window. A coincidence window is often used to minimize this and can be seen in Figure 6. To minimize the effects of these events on image quality, detector properties should be optimized to have high energy and timing resolution to reject scattered and accidental events [41], [42], [45].

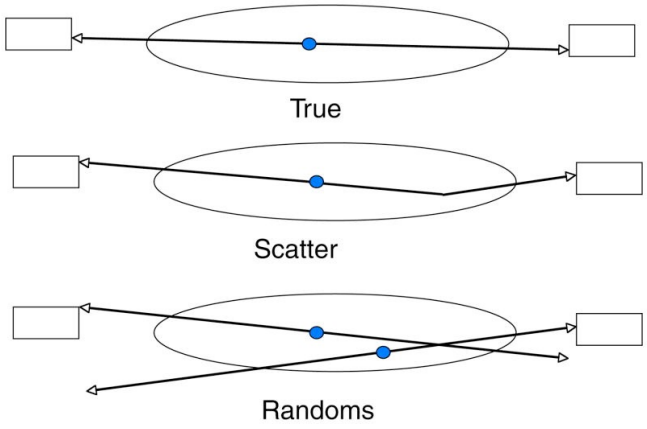

Figure 5: The three types of coincidence events. True coincidences occur when the two gamma rays from single positron annihilation are detected and neither gamma ray undergoes Compton scattering. Scatter coincidences are true coincidences where one or both of the gamma rays undergo Compton scattering before being detected. Random coincidences occur when only one gamma ray, from two independent positron annihilations, is detected within the timing window of the coincidence system [45]**.** Taken from T. K. Lewellen, 2008.

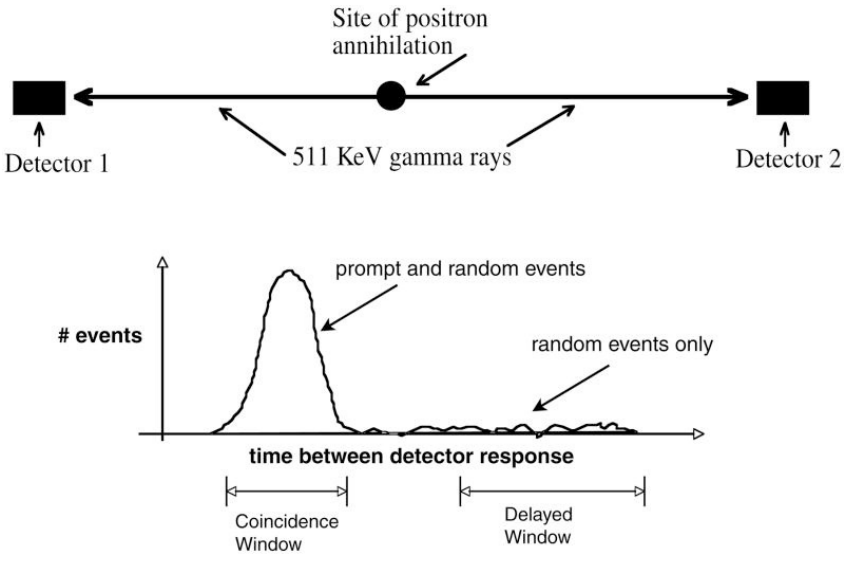

Figure 6: If a time spectrum is generated (the number of events versus the time between detector 1 and detector 2 responding), a peak is formed. This peak is usually termed the coincidence or prompt peak. During acquisition, a delayed time window can be used to measure random coincidence events [45]. Taken from T. K. Lewellen, 2008.

2.1.2 The PET Radiotracer

The usefulness of PET comes from the use of a specific radiotracer to suit the needs of the study or test. PET can be applied to numerous applications depending on the radiotracer. One of the most widely used PET tracers is ^{18}F-FDG, which is a glucose analog [42], [46]. ^{18}F-FDG is initially treated by glucose utilizing tissues in the same fashion as non-radioactive glucose (deoxyglucose or DG), and is transported into cells using the same GLUT transporter proteins. Once in the cell ^{18}F-FDG has differences from its non-radioactive form. ^{18}F-FDG is phosphorylated, to ^{18}F-FDG-6-phosphate, by hexokinase, or glucokinase in the

brain, liver, pancreas, and gut [47]–[49]. Once phosphorylated to ^{18}F-FDG-6-phosphate, it can no longer follow normal metabolic pathways or be transported out and becomes trapped in the cell; this trapping is due to the fluorine attached in place of the hydroxyl group. Only through glucose-6-phosphatase can the ^{18}F-FDG-6-phosphate leave the cell, but this mechanism is slow moving and limited. In the liver, however, due to the presence of glucose-6-phosphatase, ^{18}F-FDG-6-phosphate can be dephosphorylated and ^{18}F-FDG is released from the cells more quickly. In the fasted state hepatic glycogenolysis is activated, causing glucose-6-phosphatase to activate, releasing ^{18}F-FDG-6-phosphate into the blood as ^{18}F-FDG. Eventually, ^{18}F-FDG will again be taken up into the liver, but at a lesser quantity [50]. In tissues other than the liver, the trapping of this enzyme allows accumulation in high glucose uptake tissues, where decay can occur [46], [49], [51]. ^{18}F-FDG is only useful as a tracer to evaluate tissues with high glucose uptake, and is heavily used in oncology, since tumours have increased glucose uptake. Other tissues that have strong glucose uptake in response to treatments or conditions can be evaluated with this tracer, such as muscle, liver and adipose tissues [46].

2.2 Adipose Tissue

There are two prominent forms of adipose tissue in mammals, both of which play a role in systemic metabolic regulation within the body. White adipose tissue (WAT) is a loose connective tissue that is heavily loaded with adipocytes; these are cells that are primarily involved with the storing of triglycerides and the use of free fatty acids [52], [53]. WAT's role is heavily based on balancing caloric needs

using lipid droplets [54]. The other form of adipose tissue is BAT. BAT is a mitochondria rich tissue that is primarily responsible for non-shivering thermogenesis.

2.2.1 Distribution of BAT

Functional BAT has been known to be present in small animals and infants, but has recently been proven to be present within a large fraction of adult humans. The exact percent of individuals with active BAT is varied throughout studies, ranging anywhere from 2% to 100%. The discrepancies between studies is largely attributed to the variation in conditions and study groups; study temperature, participant age, and body mass index (BMI) all have drastic effects on the percentage of active BAT found [25]. Through the use of PET and CT, areas having above average glucose uptake, but were not tumours, were located. These regions were then identified as BAT, with depots discovered in the cervical-supraclavicular, paravertebral, and periadrenal regions. This finding opens the door for translational research from mouse models to humans, focusing on the energy balance and endocrine aspects of BAT [4], [6], [7].

2.2.2 Functions of BAT

The primary function of BAT is non-shivering thermogenesis. Non-shivering thermogenesis is the production of heat without the action of muscles shivering. It is used during mild cold exposure in adults, when mechanical shivering is not necessary. This is especially important to small animals or infants to maintain

body temperature in times of cold exposure. As illustrated in Figure 7, it occurs through uncoupling oxidation in the mitochondria. Electron transport is uncoupled from oxidative phosphorylation through the use of carbohydrates and lipids; this results in energy dissipated as heat [27], [55].

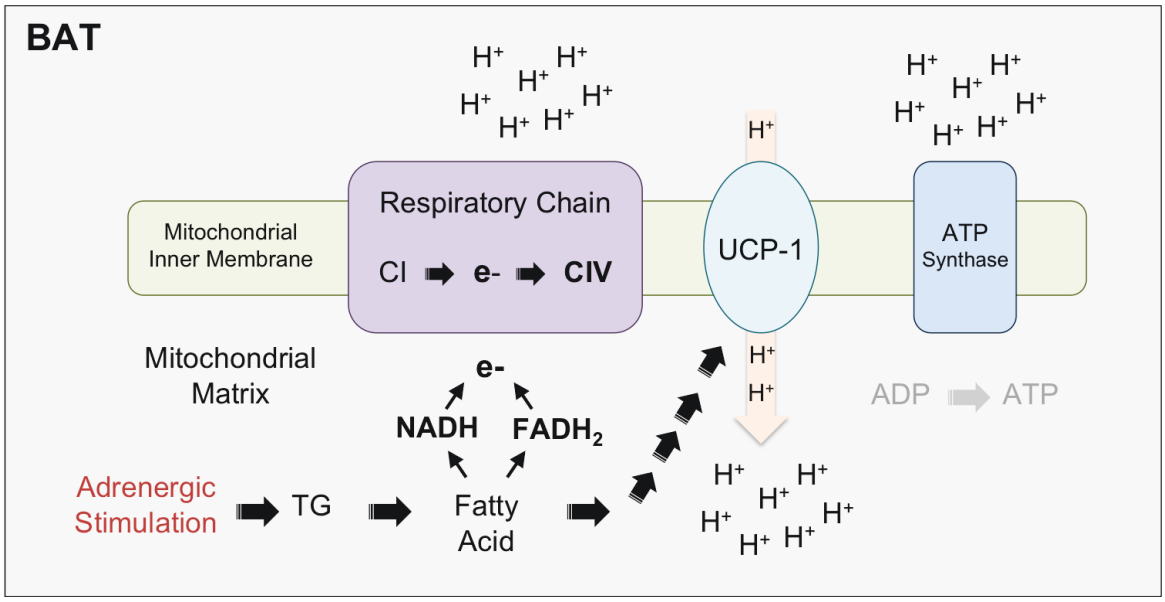

Figure 7: Method of heat production in BAT, through uncoupling protein 1. Found in the inner membrane of the mitochondria, uncoupling protein-1 (UCP-1) acts as a proton translocator. Once activated, it dissipates the proton build up across the inner membrane during oxidation. These protons are usually what drives the phosphorylation of adenosine diphosphate (ADP) to ATP, by ATP synthase, in other tissues. In the stimulated BAT, ATP synthesis is low. Fatty acids represent the main source of energy for UCP-1 and also are responsible for the formation of the electron donors in the reaction, nicotinamide adenine dinucleotide (NADH) and flavin adenine dinucleotide ($FADH_2$) [56]. Adapted from D. Richard and F. Picard, 2011

The process of uncoupling oxidative phosphorylation, also known as mitochondrial proton leak, is able to occur due to the presence of uncoupling protein one (UCP-1) within the cristae of the mitochondria [27], [57]. As a consequence lipids can be brought into the cell in order to have unrestricted oxidation. This process makes use of intracellular triglycerides as well as fatty acids from circulation. It is suggested that it is limited by the size of intracellular triglyceride stores; as oxidation occurs, triglyceride stores have been shown to deplete, limiting the level of thermogenic activity from stimulation [56], [58]. This limitation is due to the lack of triglycerides that are required for thermogenesis.

This activation of BAT can be stimulated by cold exposure, causing non-shivering thermogenesis, as well as food intake, known as diet-induced thermogenesis. Examples of stimulation causes and resulting activation are illustrated in Figure 8. Carbohydrates and other macronutrients have been shown to be activators of the sympathetic nervous system, which is the main activation pathway of BAT [7]. It is thought that BAT becomes active after a meal in order to lower metabolic efficiency and dispose of some energy as heat [23], [59], [60]. Studies in both mice and humans have indicated that a single meal can cause increased BAT blood flow, oxygen consumption, which activates the proton conductance pathway to provide an outlet for the thermic effect. It has also been noted that a single meal increases guanosine diphosphate (GDP) binding in the mitochondria, indicative of the rate of uncoupling respiration [61], [62]. Meals that are high in carbohydrates or starches as well as low in protein elicit the largest thermogenic

effect [63]. Studies suggest that norepinephrine and insulin could play a role in the diet-induced thermic effect [35], [64].

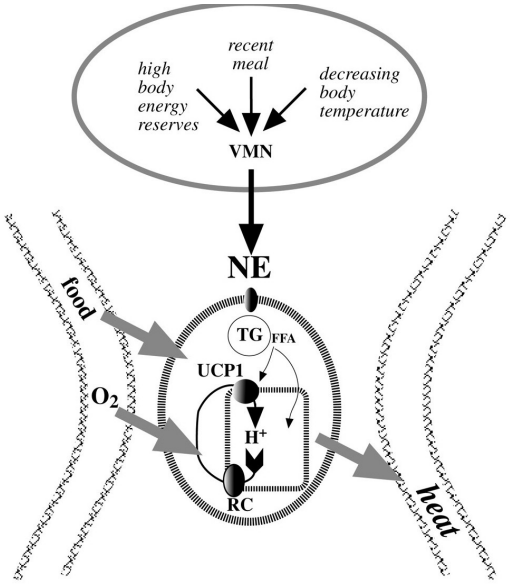

Figure 8: BAT control system. Likely through the ventromedial hypothalamic nucleus (VMN), information regarding body temperature, feeding status, and body energy reserves are coordinated. When there is a demand to increase the rate of food combustion or produce heat, the sympathetic nervous system communicates to the brown adipocytes, mainly through the β_3 adrenergic receptors, via norepinephrine (NE). This signal initiates triglyceride breakdown This releases fatty acids (FFA) from the triglycerides, which is a substrate for thermogenesis as well as a regulator of uncoupling protein-1 (UCP1) activity. Combustion of FFA in the respiratory chain (RC) allows for mitochondrial combustion of substrates. The outcome is that an increased fraction of the food and oxygen available in the blood is taken up by BAT, combusted, and leads to heat production [35]. Taken from B. Cannon, 2004.

For non-shivering thermogenesis, cold exposure activates thermogenesis in order to warm the body without the stimulation of muscular shivering. Through β_3 adrenergic receptors, brown adipocytes are stimulated by the nervous system. Following a cascade through the production of cAMP and PKA, triglycerides release free fatty acids, which provide a substrate for thermogenesis, increase UCP-1 levels as well as activity within the cell [27], [65]. Previous studies show activation in both humans, with mild cold exposure, as well as mice, with mild to extreme cold exposure, which is similar to diet-induced thermogenesis in that both mice and humans have activation due to comparable stimulus [4], [5], [66], [67]. Both activation rates, due to cold response and diet, were shown to be decreased in obese individuals. There is also an inverse correlation in brown adipose depot size and BMI; this suggests a potential role for BAT in promoting weight loss and increasing insulin sensitivity [4].

In adipose tissue it is suspected that one mechanism of insulin resistance is linked to inflammation. This inflammation is determined by the number and composition of immune cells. Macrophages, which are immune cells that contribute to adipose tissue function and normally comprise around 5% of cells within the tissue are suspected to play a role in obesity driven inflammation. In obese individuals, the percentage of macrophages increases to 50% and they begin to exhibit pro-inflammatory properties. Other immune cells have been shown to be present in adipose tissue during obesity, and the inflammation that is

linked to these has been correlated to whole body insulin resistance along with adipose tissue insulin resistance [39]. BAT has been shown to be more resistant to this inflammatory response during obesity, but is not entirely immune, showing inflammation after longer-term high fat diets [40].

BAT has also been shown to have endocrine features along with being responsible for non-shivering thermogenesis. It has been suggested that BAT releases endocrine factors such as insulin-like growth factor 1, interleukin-6, and fibroblast growth factor-21. These factors are released during thermogenic activation [9]. The suggestion of this role was made after mice with genetically ablated BAT, through the use of UCP-1 promoter-driven diphtheria toxin, were shown to suffer from more metabolic effects than those related to just thermogenesis including hyperphagia, obesity, hyperglycemia, insulin resistance, and hyperlipidemia [68], [69]. These adverse effects are hypothesized to be related to glucose metabolism of BAT, due to the tissue being a large consumer of glucose.

2.3 Glucose Metabolism

Glucose metabolism provides energy that is normally utilized by many organs throughout the body. Other sources of energy, such as fat or protein, can also be utilized, but many tissues require glucose, and the nervous system normally requires glucose as an energy source. Acquired primarily through diet, glucose is essential for many bodily functions [70].

2.3.1 Digestion and Absorption of Glucose

In normal instances, glucose uptake within tissues would begin through entry in the gut, following a meal. Glucose, being a monosaccharide, is able to cross the brush border of the intestines through diffusion, but this process is slow. The predominant method of transport into the enterocytes of the gut is a carrier-mediated mechanism. A sodium (Na^+) dependent glucose transporter binds with the glucose as well as Na^+ at different sites. Due to a higher concentration of sodium ions within the gut lumen compared to the interior of the enterocyte, sodium travels down the concentration gradient into the cell, bringing glucose with it. This glucose is then transported out of the cell into circulation through the transport protein GLUT-2 [70].

2.3.2 Glucose Uptake of the Pancreas and Insulin Release

After a meal dietary glucose quickly reaches the pancreas. Glucose is transported into pancreatic β-cells through GLUT-2, and is phosphorylated by glucokinase. This causes glucose metabolism to be stimulated, resulting in an increased ATP/ADP ratio within the cell. Due to this increase, the ATP sensitive potassium channels in the membrane close, causing the cell to depolarize and voltage dependent calcium channels to open. Calcium passes through this channel into the cell, activating calcium-dependent kinases, which stimulate insulin release from the cell into circulation. Once in circulation insulin acts on a number of tissues [70].

2.3.3 Glucose and Insulin Action on the Liver

When glucose enters circulation it also encounters the liver, where it once again comes across GLUT-2, which allows it to enter the hepatic cells. Inside the hepatocyte glucokinase converts the glucose to glucose-6-phosphate, causing glucose to enter all the major glucose metabolism pathways: glycolysis, the pentose pathway, and glycogenesis. The primary role of glucose in the liver is glycogenesis, which causes the production of glycogen, a polysaccharide storage form of glucose. The most concentrated store of available glycogen is in the liver, which is used in-between meals to maintain blood glucose levels, through glycogenolysis. In skeletal muscle, glucose is also converted to glycogen, but the primary use for this glycogen is energy metabolism, instead of blood glucose maintenance. The liver is also affected by circulating insulin, released by the pancreas after a meal. Circulating insulin binds to the insulin receptor, causing it to autophosphorylate, leading to phosphorylation of insulin receptor substrates (IRS) and adaptor proteins. Next, PI3K is activated which leads to Akt activation. In the liver specifically, this phosphorylation of Akt causes GSK-3β to phosphorylate and become inactive. This leads to the storage of glucose as glycogen. Insulin also blocks gluconeogenesis and glycogenolysis in the liver which inhibits the production and release of glucose [70].

2.3.4 Glucose and Insulin Action on Skeletal Muscle

Like the liver, skeletal muscle stores glycogen, but due to the lack of a glucagon receptor or glucose-6-phosphatase it cannot be released to maintain blood

glucose levels. Instead skeletal muscle glycogenolysis is activated in response to epinephrine or during physical activity [71], [72]. Skeletal muscle also responds to insulin stimulation similarly to the liver through the insulin receptor leading to phosphorylation of Akt; at this point however, the increase in Akt activity causes the glucose transport protein GLUT 4 to translocate from inside the cell to the membrane. This facilitates the uptake of glucose into the cell; leading to glycogen synthesis for storage, as well as glucose metabolism processes, and the influx of amino acids aiding in protein synthesis [70].

2.3.5 Glucose and Insulin Action on Adipose Tissue

Both WAT and BAT are responsive to insulin and glucose, but differ in some minor ways. BAT is similar to skeletal muscle in insulin signalling from the IR, leading to IRS-1 and insulin receptor substrate 2 (IRS-2) phosphorylation. IRS-1 phosphorylation causes Akt activation, IRS-2 phosphorylation causes binding to a subunit of PI3K. The increase in Akt activity causing GLUT 4 to be translocated to the cell membrane and glucose be transported into the cell. This pathway is similar to that of WAT, except that BAT contains a higher amount of GLUT 4 and in turn is more responsive to insulin than WAT. There is also an IR dependent, but PI3K independent pathway that has been shown to cause GLUT4 translocation. This pathway is thought to initially act by recruiting the proto-onco protein Cbl (Cbl) to the activated IR through adapter proteins c-Cbl associated protein (CAP) and adapter protein with Plekstrin homology and Src homology domain (APS). APS becomes phosphorylated by IR, leading to the

phosphorylation of Cbl, causing Cbl association with CAP and CT10-related kinase (CrkII). Through the lipid raft protein flotillin TC10 in lipid rafts is activated. TC10 binds to a number of downstream effectors, all of which have roles in actin dynamics. Actin cytoskeleton reorganization is critical in GLUT4 vesicle tracking and translocation to the plasma membrane. This pathway can also be responsible for insulin stimulated glucose uptake through GLUT 4 [73]. Either of these pathways will lead to glucose entry to the cell. After entering the cell, glucose stimulates de novo fatty acid synthesis and the synthesis of triglycerides. It can also be stored as glycogen, which will occur when animals are warm and BAT is not generating heat. BAT is one of the most insulin responsive tissues, with respect to stimulated glucose uptake and has been shown to have an effect on whole body insulin sensitivity, making it an ideal target for new T2D therapies [35].

2.3.6 Pathogenesis of Insulin Signalling

T2D is a syndrome that affects fuel metabolism and is characterized by hyperglycaemia leading to neural and vascular complications. The development of T2D is strongly linked with genetic factors, however lifestyle factors, such as poor diet, obesity, and physical inactivity, often unmask the disease. Age is also a factor as most patients who develop T2D are over 40 years of age. The pathogenesis is a combination of insulin resistance leading to impairment of insulin secretion in its final stages. Initially insulin resistance presents as hyperinsulinemia, but with a normal glucose concentration. The increasing levels

of insulin will at one point become insufficient to offset the tissue resistance and an increase in glucose concentration during fasting can result; this is known as impaired fasting glucose. There can also be an impairment during high glucose intake, known as impaired glucose tolerance (IGT). Eventually, a further insulin resistance leading to impairment of insulin secretion leads to T2D development. This development process can take years to develop and if aware of the early changes, the development can be slowed or in some cases reversed [70].

Tissues can be susceptible to insulin resistance, primarily insulin sensitive tissues. Insulin sensitive tissues are ones that, in response to insulin, will take up glucose from the blood stream. These tissues include, but are not restricted to, skeletal muscle, both BAT and WAT, the heart, and the liver. In diabetic or insulin resistant individuals, some of these tissues display tissue specific insulin resistance. In cardiac tissue the exact mechanism for insulin resistance has not been elucidated. Insulin resistance in heart tissue is often associated with diabetes and heart diseases [74], [75]. Sixty-five percent of people with T2D die from a form of cardiovascular disease and stroke [76]–[78]. In skeletal muscle, adipose tissue, and liver, insulin resistance occurs due to dysfunction in a signalling process post IR phosphorylation, but not all methods of action are known. In skeletal muscle it is suspected that a mitochondrial oxidative potential is impaired in individuals with T2D and in obese individuals with insulin resistance, but who are not diabetic. It is suggested that skeletal muscle insulin resistance is an early indicator and linked to T2D development [79].

Understanding tissue specific insulin resistance and how it plays into whole body insulin resistance is important for understanding treatment and prevention.

2.3.7 Complications and Effects

The most common acute complication of T2D is hypoglycaemia, which is a result of an imbalance between circulating insulin levels, carbohydrate supply, and physical activity. The cause of this can stem from an incorrect dose of insulin or missing a meal, in severe late stage T2D. Another consideration is the amount of exercise, since physical activity increases the insulin-independent tissue glucose uptake. The severity of hypoglycaemia can vary from mild, which can be managed with glucose rich foods, or sever which requires medical attention [70].

Ketoacidosis is another potential side effect of T2D. Although not common, it is a severe medical emergency. It can develop rapidly in individuals with T2D after a major metabolic stress, such as a myocardial infarction. Ketoacidosis is when there is an excess of acetyl-CoA, which is a substrate for the production of ketone bodies. This increases the amount of ketone bodies in the plasma. The overproduction of acetoacetic and β-hydroxybutyric acid increases the blood hydrogen ion concentration, or in other terms causes a pH decrease. It can become life threatening if left untreated [70].

The most common life threatening complication of diabetes, however, is cardiovascular disease. It is the main cause of death among people with T2D. It

is linked with metabolic syndrome, which is the cluster of dyslipidemia, increased arterial blood pressure, obesity, insulin resistance, and glucose intolerance. Metabolic syndrome is also linked with low-grade inflammation, which affects the vasculature, and an increased tendency to thrombosis [70]. The common denominator between all these risk factors for cardiovascular disease is still not completely known, but T2D and cardiovascular disease are strongly related and may share common genetic and environmental antecedents [79].

2.4 PET for Assessing Tissue Specific Glucose & Insulin Kinetic Changes

Due to the relation between T2D, early indications of tissue specific insulin resistance, and cardiac disease, research in the linkage of these conditions and progression continues to be undertaken. As well as whole body effects and relations, tissue specific linkages and risk factors are being looked at, mainly in muscle, BAT, and cardiac tissue. Due to the insulin sensitivity of these tissues of interest, PET shows promise as a method to investigate tissue specific glucose/ insulin kinetic changes related to T2D.

2.4.1 Insulin Resistance Linked Cardiac Conditions

Whole body insulin resistance has been linked to multiple diseases of the heart such as chronic heart failure (CHF), hypertrophy, coronary artery disease (CAD), myocardial infarction, and idiopathic dilated cardiomyopathy (IDCM) [74], [80]–

[82]. In all of these tissues a decrease in cardiac tissue specific glucose uptake, both insulin stimulated and basal, has been found. Studies have also suggested that myocardial insulin resistance may be the cause of, or play a role in, the development of some of these disorders. Specifically it has been suggested that myocardial insulin resistance may cause CAD, IDCM, and CHF [74], [75]. Furthermore, a relationship between severity of insulin resistance and the severity of heart disease has been shown. Meaning increased insulin resistance is shown to correlate to worsened heart failure and a lesser survival time [75], [81]. These findings make a case for studying early indications of insulin resistance in cardiac tissue.

2.4.2 Cardiac Tissue Study Methods

Unlike BAT, which came into interest with the advent and use of PET, cardiac tissue has been studied prior with various *ex vivo* methods. The main methods used are perfusion and cell culture models. Perfusion models generally involve the use of a Langendorff apparatus, which has been in practice since 1897. Although it has evolved since its initial conception, the term can be used to describe numerous variations of heart perfusion. The Langendorff perfusion model's complete method description can be found in Skrzypiec-Spring et al. [83]. To summarize, the heart of the animal is attached to a cannula on the apparatus, which provides oxygenated perfusion solution, which is kept at 37°C and gassed with 5% CO_2 in order to maintain a physiological pH of 7.4. This solution will perfuse the entire ventricular mass of the heart and exit via the

coronary venous circulation. This apparatus is often water-jacketed to maintain a temperature of 37°C for all components.

This system has been used to study isolated heart tissues and has provided valuable information about heart function. The method continues to be used due to the reproducible results, ease of use, and low cost [83], [84]. The method provides information about physiological, morphological, biochemical and pharmacological parameters including contractile function, heart rate, coronary vascular function, cardiac metabolism, morphology and electrical activity. The downside of the method is that the heart has been removed from the body and all outside signalling has been removed. There are also a number of outside factors and differences between the perfusion model and an *in vivo* heart that can impact results. The heart is also sensitive to contusion injuries while connecting to the apparatus, as well as contamination once connected. The main issue, however, is the degradation of the heart over time. It has been reported that there is a 5%-10% reduction in heart function every hour [84], [85]. Also, due to the lack of outside factors and signalling this model can fail to be completely physiological when studying endocrine related systems.

The second method currently used is a cell culture model. In these models cardiomyocytes are commonly used. Cardiomyocyte isolation and culture was developed many years ago and has provided great insights into response to drugs and conditions. These cells are collected from various species, including

humans. Immortalized cell lines, which can be used instead of primary cell collections, also exist. Cell culture models provide an isolated microscopic view of the heart system and responses. They provide the ability to change conditions of growth or investigate responses to added drug treatments easily without outside bodily functions affecting response. The downside of this method is similar to the perfused heart models; outside signalling events and responses of other areas of the body to the heart cannot be measured or taken into account [85]–[87].

2.4.3 Cardiac Specific PET

In order to overcome the obstacles of the models in use for cardiac insulin sensitivity, an *in vivo* method would be advantageous. Due to recent advancements, PET is being investigated as an *in vivo* analysis method and alternative to perfusion and cell culture models. PET imaging provides a non-invasive alternative, which does not require removal and potential damage to the heart. All endocrine signalling and effects from other tissues remain, in order to provide a more physiological view of treatments. Through the use of ^{18}F-FDG, glucose uptake can be measured in the heart tissue specifically and the results of treatments or diseases on this uptake can be compared.

2.4.4 BAT Study Methods

Like previously mentioned BAT came into the spotlight with the advent and advancement of PET, however other methods of studying the tissue are often

used. Some of these methods include cell culture of brown adipocytes, thermography, histology, and the use of 2-deoxy-D-[H^3] glucose (2DG) followed by euthanasia, tissue collection, and glucose/radiation level measurement [25], [26], [88]. Methods involving cell culture of brown adipocytes, like cell culture models of cardiac tissues, allow for a simplistic view of responses to treatments, however lack the effects of other tissues and responses in the body or environment, which could play a major role in BAT response in humans. Thermography provides BAT temperature, which is linked to activation, but does not provide information regarding intracellular function or pathways of activation. It is also unknown if temperature changes between individuals are consistent with a similar level of activation. Histology and 2DG use do not allow for repeated measures from the same animal, since tissue collection is required to perform the experiments. 2DG use however, does allow for quantifiable uptake values, and the potential for un-anesthetized treatment and glucose uptake periods [26].

2.4.5 BAT Specific PET

PET is widely used for BAT glucose uptake research, particularly using ^{18}F-FDG as the radiotracer of choice. Using PET to research BAT has the advantage of providing quantifiable values of glucose uptake in the specific tissue, while still providing complete interaction between BAT and other components of the body. The added benefit of PET over other methods, such as 2DG uptake analysis, is that PET can be performed multiple times on the same animal and does not require euthanasia for measurement of results. It also allows for real time uptake

through the use of dynamic scans, however this does require anesthesia. There are also other radiotracers that are being developed or used to measure other processes in BAT, such as 4-18F-fluorobenzyltriphenyl phosphonium (^{18}F-FBnTP), which targets the electrochemical gradients and accumulates in mitochondria as a function of their uncoupling state [88]. Continued development of PET tracers and methods will allow PET to remain one of the best methods for assessing BAT activity and/or glucose uptake.

2.4.6 Skeletal Muscle Study Methods

Similar to BAT and cardiac muscle, skeletal muscle can be studied using cell culture models. These models are quite prevalent, and provide a way to assess the action of many specific compounds and muscles from different species and locations. The cells can be primary cells isolated from an animal or human or from an immortalized cell line. Primary cells in theory provide a better representation of muscle in the body and should have more similar characteristics. These cells however, have a shorter life span in culture than cell lines and only a finite number can be collected from one individual, leaving variation among animals as a factor in studies. Cell lines are more likely to be consistent between sets and can be cultured for longer. They may have different characteristics or changes that have occurred since they are not directly isolated from the source each time, but rather continually cultured. Both of these methods however, do not allow for a whole picture of the body and processes that may have an effect on the muscle *in vivo*. Another method of study is tying a muscle

up in a bath. This is similar to what was described for cardiac tissue, and allows for the use of various bath conditions surrounding the muscle, stimulation from electricity to simulate contraction, and the measurement of channel currents using patch clamps [89]. Once again the downside to this method is the lack of outside factors that may play a role in the response of the muscle, as well as the potential damage to the muscle due to surgical procedures [90].

2.4.7 Skeletal Muscle Specific PET

Similar to cardiac muscle PET, skeletal muscle PET would benefit research in the area by allowing *in vivo* analysis of animals and individuals. This would allow for other factors and stimulus to be accounted for in studies, since the muscle of interest would remain intact. This would also allow repeated measurements on the same subjects, since euthanasia is not required to assess glucose uptake, or uptake using other radiotracers that measure different metabolic pathways. This also removes the risk of damage to the muscle tissue that can occur during removal and the tying up procedure. Current literature using PET to analyze skeletal muscle has been able to show response of muscle to insulin, dietary state, temperature, as well as differences between healthy and T2D subjects in response to insulin [82], [91]. It has been confirmed that both dynamic and static PET imaging give similar results in insulin stimulated glucose utilization, and would both be good tools for skeletal muscle insulin resistance tests [92]. It has also been demonstrated using the radiotracer [^{11}C] palmitate, that obesity is characterized by elevated fatty acid oxidation and a slow fractional transfer of

fatty acids into triglycerides in skeletal muscle [23]. These findings prove the usefulness of PET in skeletal muscle, with the use of ^{18}F-FDG or other tracers that have or will be developed.

3. Methodology and Experimental Design

3.1 Institutional Animal Care Approval

All animal experiments were performed in accordance with the institutional animal care committee guidelines at Lakehead University. C57BL/6 male mice were obtained from Charles River Laboratories Inc. at 6-8 weeks of age. Mice were housed in Innovive disposable cages (Innocage®) with the pre-filled bedding replaced with All Living Things® Small Pet Bedding. A small amount of bedding from the mouse transport box was added to cages to help with adjustment. Mice had access to water and food at all times, except where otherwise stated. Food was LabDiet 5001 Rodent Diet (Land of Lakes Inc., Arden Hills, Minnesota, U.S.A.). Mice were housed in Innovive Innorack® IVC mouse racks. Enrichment was provided with plastic enrichment domes in each cage. Mice were acclimatized after arrival for at least one week before experiments begin. Housing temperature and humidity levels were controlled, at 22°C ± 3°C and 50% ± 9% respectively, mice were kept on a 12hr light/dark cycle.

3.2 Experimental Protocol

3.2.1 Limitations and Basic Assumptions

Animal models are often used to represent a better environment for testing physiological treatments, compared to cell culture models. In this study an animal model is used for all experiments. The first limitation is that one strain of mouse is used exclusively, C57BL/J mice. This strain is an inbred normal mouse, no other strains of mice are used in the study and it is assumed that this strain of mouse represents healthy normal physiological conditions. It is also assumed that these mice are in good health and lack any pre-existing conditions, health reports from the vendor are provided, but do not account for all physiological conditions. Another limitation related to animal models is the environmental factors that can unknowingly affect the animal. All mice are kept in the same environment, but some small uncontrollable variations may occur. The extent of the effect these variations may have is not known, neither is it known if they will relate to the area of interest of the study. It is also assumed that these mice will consume the same amount of food and water and remain well hydrated and fed, except during fasting time periods, as well as that there are no differences amongst the mice that would alter the outcome of the experiments. It is also assumed that the G4 microPET system was operating properly and results from this equipment are accurate.

3.2.2 Delimitations

Image analysis was performed by a single individual. Due to the nature of the analysis software some amount of personal judgement is needed. A single individual was used to analyze the data to limit variation between the personal judgement of individuals and keep the style consistent. Using a single individual does not allow for comparison to account for any bias or skew, but due to the issues with consistency, time constraints, and lack of available personnel it was decided that one individual would perform the analysis exclusively.

3.2.3 Treatments

To asses BAT glucose uptake and signalling, treatments given were either a control with no accompanying injections in addition to ^{18}F-FDG, 60mg dextrose (2g/kg bodyweight) (Fischer, Whitby, Ontario, Canada) made to 100µl in cell culture grade water, 1.2mg L-leucine (40µg/g bodyweight) (Sigma Aldrich, Oakville, Ontario, Canada) made to 100µl in cell culture grade water (Leucine), 60mg dextrose treatment + 1.2mg L-leucine treatment (Glucose + Leucine), or 1.3mg L-glutamic acid (45µg/g bodyweight) (Sigma Life Science, St. Louis, Missouri, U.S.A.) made to 100µl in cell culture grade water + 60mg dextrose treatment (Glutamic Acid + Glucose).

To assess inhibition of β-adrenergic action, above treatments were repeated with an additional injection of 150µg/mouse of propranolol hydrochloride (St. Louis, Missouri, United States of America).

To asses cardiac uptake, treatments of 10U/kg insulin (humulin (Eli Lilly Canada), Toronto, Ontario, Canada) with 60mg dextrose were given with the ^{18}F-FDG.

3.2.4 Static Image Acquisition

At least five days prior to experiments mice were individually housed, a handful of bedding from the original group housed cages was added to the individual cage to help with adjustment.Five to seven hours prior to experimentation mice were placed into clean cages, with no food for the fasting period, but free access to water. Mice were transported to the experimentation room, where a constant temperature was maintained (22°C ± 1°C) for the course of the experiments.

^{18}F-FDG (2-deoxy-2-(18F)fluoro-D-glucose) (Center for Probe Development and Commercialization, Hamilton, Ontario Canada) was obtained on experiment days. Following the “FDG Dilution Worksheet” (see appendix) a concentration of approximately 200μCi/ml of ^{18}F-FDG diluted with sterile saline was made. A mouse was anesthetized with 2% isoflurane anesthetic (Fresenius Kabi Canada (formerly PPC), Richmond Hill, Ontario, Canada) for three minutes inside a vapour induction chamber. At this time intraperitoneal injections of the volume of diluted ^{18}F-FDG to provide a dose of approximately 20μCi were given. Any other treatments were also given with an intraperitoneal injection. A fifteen-minute wait time existed between treatment injections of each subsequent mouse to avoid scan time overlap. One hour after treatment injection, mice were anesthetized with 2% isoflurane again for three minutes. Mice were then placed in the imaging

chamber in prone position and inserted into the G4 PET/X-Ray scanner (Sofie Biosciences, Culver City, California, United States of America). The imaging chamber contains a nose cone for isoflurane administration and the bed was heated to 37°C. Image acquisition proceeded for ten minutes. In this imaging time isoflurane anesthesia was lowered to 1.5% to reduce dose, while maintaining lack of consciousness. Each mouse was subsequently imaged under the same parameters one hour after the treatment injections. After the scan was completed an x-ray was performed as per the specifications of the G4 scanner. Once the x-ray is complete mice were returned to fasting cages to recover from anesthesia. After experimentation mice were returned to original cages, used prior to fasting, and food was returned.

3.2.5 Dynamic Scan Acquisition

For preliminary analysis to determine scan time dynamic scans were completed. Visual depictions of the results are found in the appendix. The dynamic scan was completed following the same protocol as the static scanning, with the following differences. A one hour fifteen-minute wait time existed between treatment injection of each subsequent mouse to avoid scan time overlap. Immediately after treatment injection, the mouse was placed in the imaging chamber (37°C heated bed) in the prone position, with its nose inserted into the nose cone to ensure isoflurane inhalation. The imaging chamber was placed in the G4 PET/X-Ray scanner and a 70 minute acquisition performed (7x600). During the initial five minutes of the scan the isoflurane was lowered to 1.5%.

After the scan was completed an x-ray was performed as per the specifications of the G4 scanner. The mouse was then moved back to its fasting cage, which was placed on a heating pad (37°C) to help recovery from anesthetic. Upon completion of experiments, mice were returned to their original cages used prior to fasting.

3.2.6 Image Analysis

VivoQuant™ (Version 1.23, invicro, Boston) image analysis software was used to reconstruct and quantify uptake values within specific tissues. Regions of interest were selected to encompass a specific tissue. A volume of the entire tissue was drawn using a spherical draw tool. Once the entire tissue was encompassed standardized uptake values (SUV) as well as SUV_{MAX} were calculated.

$$SUV = \frac{\frac{Activity\ in\ region\ (\mu Ci)}{region\ volume\ (ml)}}{\frac{Injected\ dose\ (\mu Ci)}{Body\ weight\ (g)}}$$

SUV was reported in g/ml, SUV_{MAX} was reported in SUV/mm^3. SUV_{MAX} is the calculated SUV on the image pixel that has the highest SUV in the region of interest. Tissues analyzed were bladder, heart, tongue, harderian glands, interscapular brown adipose tissue (IBAT), which was chosen due to the size, ease of visualization, and lack of surrounding tissue interference, paraspinal muscles, and a combined region containing biceps brachii and triceps brachii also called the upper forelimb skeletal muscle (UFSM). SUV and SUV_{MAX} were

calculated for each tissue for each treatments group, as long as the tissue was visible.

Analysis of dynamic scans were completed in a similar way to the static scans, except regions of interest were drawn over tissues in all time intervals used. For a 7x600 scan, seven 10 minute intervals were analyzed.

3.2.7 Statistics

Outliers were identified as greater than 1.5 times the interquartile distance above the third quartile or less than 1.5 times the interquartile distance below the first quartile, which is the standard SPSS outlier definition. Significance was determined using a one-way fixed effects ANOVA with a Fischer LSD post-hoc with Bonferroni correction.

3.2.8 Tissue Collection

Mice were fasted for 5hr, then treatments of Control, Glucose, Leucine, Glucose + Leucine, and Insulin were administered to the intraperitoneal cavity. State of temperature and wakefulness were determined by comparing static and dynamic imaging results for optimal conditions. Fifteen minutes after injection of the Insulin treatment, and 30 minutes after the injections of all other treatments mice were anesthetized under 5% isoflurane anesthetic and the hearts removed. IBAT and soleus muscle were then removed and immediately frozen on dry ice for future analysis.

3.2.9 Tissue Lysis

Frozen IBAT was homogenized in ice-cold lysis buffer (25mmol/L Tris pH = 7.5, 150 mmol/L NaCl, 1 mmol/L EDTA, 1% Triton-X 100) with an addition of Sodium Fluoride (NaF) (Sigma Life Science, St. Louis, Missouri, U.S.A.) and Protease Inhibitor Cocktail (Sigma Life Science, St. Louis, Missouri, U.S.A.). Homogenization was completed using the Qiagen TissueLyser. Samples were then centrifuged at 16000 g for 10 minutes at 4°C, supernatants were then collected and stored at -80°C until further analysis could be completed. Protein assays were completed (Pierce™ BCA Protein Assay Kit, Thermo Scientific, Rockford, Illinois, U.S.A.) in order to determine protein content for western blot analysis.

3.2.9 Western Blotting

Protein was loaded and resolved by SDS-PAGE on 10% polyacrylamide gels, and transferred to nitrocellulose membranes. Immunoblotting was performed using the primary antibody: anti-AKT(phosph S473) (Abcam, 66138, Cambridge, MA, USA), Akt (pan) (C67E7) (Cell Signalling Technology, 4691, Danvers, MA, USA) , Anti-GSK3 beta [3D10] (Abcam, AB93926, Cambridge, MA, USA), Phospho-GSK-3β (Ser9) (D85E12) XP® Rabbit mAb (Cell Signalling Technology, 5558, Danvers, MA, USA), and UCP1 (D9D6X) Rabbit mAb (Cell Signalling Technology, 14670, Danvers, MA, USA). After incubation the secondary antibody: Pierce antibody Goat-anti rabbit IgG (H + L) (Thermo Scientific Pierce, 31460, Rockford, IL, USA) was used, except for the case of Anti-GSK3 beta [3D10], in

which the secondary antibody Stabilized Goat anti-Mouse IgG (H+L) Peroxidase Conjugated (Thermo Scientific, 32430, Rockford IL, USA) was used. Detailed steps can be found in the Lees lab SOP for Western Blotting (see appendix). The immunoreactive complexes were detected with enhanced chemiluminescence (ChemiDoc^{TM} XRS, Bio-Rad, Hercules, CA, USA) and quantified using ImageJ software.

4. Results

4.1 Modulation of Glucose Uptake in BAT

4.1.1 Glucose Treatment Increases Glucose Uptake in BAT

Mice that were given treatments of 2g/kg glucose one hour prior to a 10minute PET scan exhibited increased ^{18}F-FDG uptake in IBAT compared to control mice. This increase is represented as an increase in both SUV and SUV_{MAX} in the region, compared to control (Figure 9).Glucose-stimulated ^{18}F-FDG uptake was not observed in any of the other tissues examined (Figure 10). In forelimb skeletal muscle and heart no change was observed, compared to control (Figure 10). However, a significant decrease in ^{18}F-FDG SUV_{MAX} was seen in harderian glands and tongue and a significant decrease in SUV was seen in harderian glands (Figure 9).

4.1.2 Leucine Potentiates Glucose-Stimulated ^{18}F-FDG Uptake in IBAT

When 40μg/g body weight leucine was given to mice, glucose uptake in IBAT exhibited a non-significant decrease of 11% compared to control mice (Figure 9). However, when the leucine treatment was given in combination with the glucose treatment, a significant increase in glucose uptake in IBAT was seen compared to control (Figure 9). In fact, ^{18}F-FDG uptake was also higher than that seen with the glucose treatment alone. In the other tissues analyzed, leucine alone produced no significant changes in glucose uptake from control. However, a significant decrease in ^{18}F-FDG uptake was observed in harderian glands following glucose alone and glucose and leucine in combination, compared to control. The changes in ^{18}F-FDG uptake are represented as both SUV and SUV_{MAX} in the region respectively (Figure 10).

4.1.3 Glutamic Acid Does Not Increase Glucose Uptake in BAT

When mice were given the 45μg/g bodyweight of glutamic acid with 2g/kg glucose treatment, there was no increase in ^{18}F-FDG uptake in IBAT observed (Figure 11). Similarly, no differences were observed in the heart and paraspinal skeletal muscle, however, significant decreases were observed for the harderian glands (SUV and SUV_{MAX}), upper forelimb skeletal muscle (SUV_{MAX}), and tongue (SUV and SUV_{MAX}) ($p \leq 0.05$).

4.2 Leucine and Glucose Treatment Increases Glucose Uptake Through an Adrenergic Dependent Pathway

In order to determine if Leucine + glucose-stimulated ^{8}F-FDG was acting through adrenergic signalling, a beta blocker, propranolol, was used. A significant decrease in ^{18}F-FDG uptake was observed in IBAT following pretreatment with propranolol (Figure 12) ($p \leq 0.05$). While insulin + glucose was able to increase ^{18}F-FDG compared to control, pretreatment with propranolol before insulin + glucose did not prevent this effect (Figure 12) ($p \leq 0.05$). These data indicate that insulin + glucose mediate ^{18}F-FDG uptake is not dependent on adrenergic signalling. However, pretreatment with propranolol before leucine + glucose did prevent any increase in ^{18}F-FDG uptake, indicating that adrenergic signalling is required for leucine + glucose mediated ^{18}F-FDG uptake (Figure 12)($p \leq 0.05$). The other tissues analyzed are shown in Figure 13. Of note, the heart demonstrated an ~3-fold increase in ^{18}F-FDG uptake as a result of insulin + glucose treatment ($p \leq 0.05$), which was not prevented with propranolol pretreatment.

4.2.1 Glucose And Insulin, Either Alone Or In Combination, Did Not Produce Detectable Changes In insulin Signalling.

In order to assess the effect of the various treatments on insulin signalling, IBAT and soleus (hindlimb skeletal muscle) were collected following treatment and western blots for pan and p-Akt and pan and p-GSK-3β were performed. The

soleus served as a control tissue since insulin mediated signalling is well known for this tissue. As expected, insulin resulted in elevated p-Akt/pan-Akt ratios (Figure 14) ($p \leq 0.05$). Insulin also increased the p-Akt/pan-Akt ratio for IBAT (Figure 15) ($p \leq 0.05$). Unexpectedly, insulin did not cause increased p-GSK-3β/ GSK-3β ratios in either IBAT or soleus. Glucose and leucine, either alone or in combination did not cause an increase in the p-Akt/pan-Akt ratio, indicating that these treatments did not increase ^{18}F-FDG uptake. However, it is possible that any increase in the insulin signalling through Akt and GSK-3β were too small to be detected via western blots.

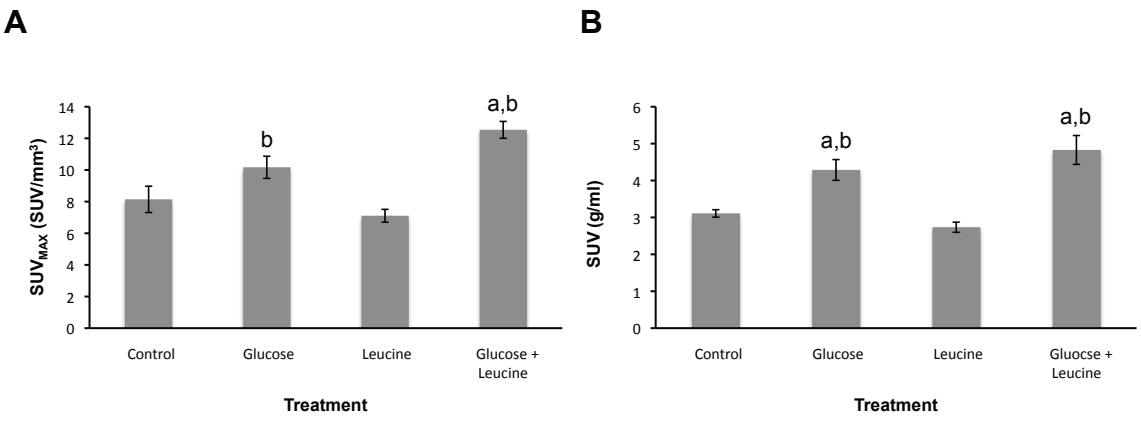

Figure 9: A 10 minute static PET scan was completed, SUV and SUV_{MAX} were measured to determine changes in glucose uptake in IBAT. Treatments Glucose (2g/kg bodyweight), Leucine (40µg/g bodyweight), and Glucose & Leucine (2g/kg bodyweight glucose & 40µg/g leucine). A) SUV reported in g/ml, analyzed using a region of interest encompassing the entire tissue. B) SUV_{MAX} reported in SUV/ mm^3, analyzed using the same region of interest as SUV calculations, but with the pixel with the highest uptake used for determination of the value. “a” denotes a significant change from control, “b” denotes a significant change from leucine ($p<0.05$ for all). n=6-8, if tissue was not visible in scan image it was excluded.

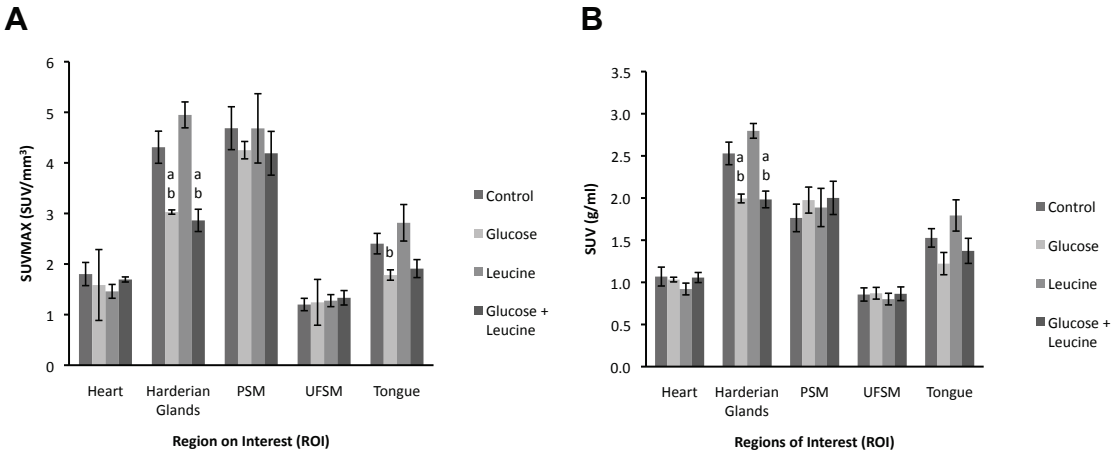

Figure 10: A 10 minute static PET scan was completed, SUV and SUV_{MAX} were measured to determine changes in glucose uptake in the heart, harderian glands, skeletal muscle (represented as paraspinal (PSM), and upper forelimb (UFSM), and the tongue). Treatments Glucose (2g/kg bodyweight), Leucine (40µg/g bodyweight), and Glucose & Leucine (2g/kg bodyweight glucose & 40µg/g leucine). A) SUV_{MAX} reported in SUV/mm^3, analyzed using the same region of interest as SUV calculations, but with the highest uptake pixel used for determination of the value. B) SUV reported in g/ml, analyzed using a region of interest encompassing the entire tissue. “a” denotes a significant change from control, “b” denotes a significant change from leucine ($p<0.05$ for all) n=4-8, if tissue was not visible in scan image it was excluded.

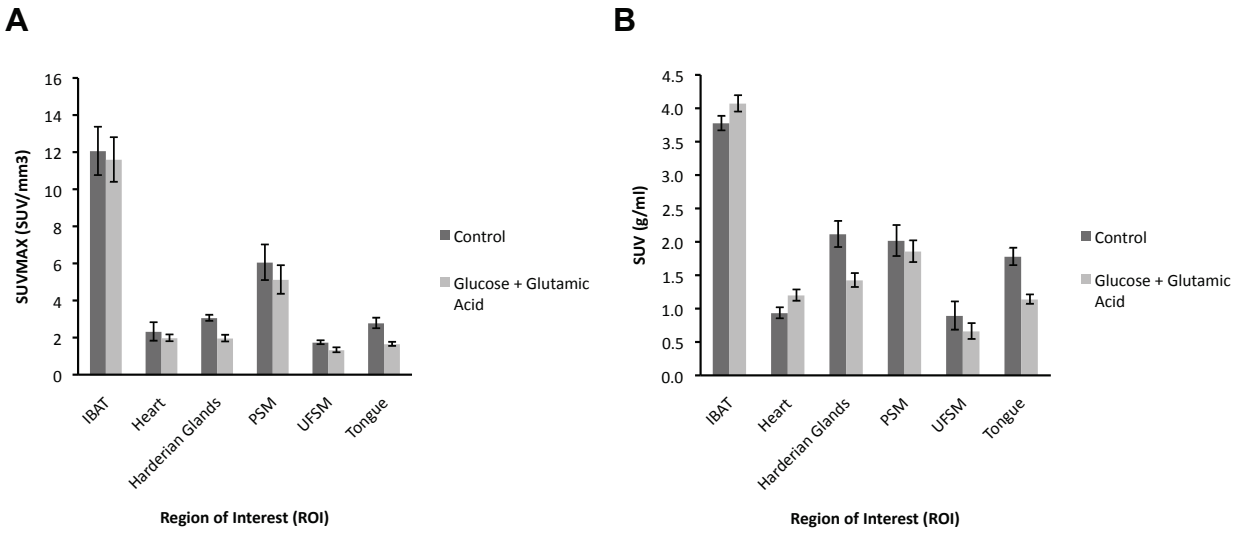

Figure 11: A 10 minute static PET scan was completed 1hr after injection with the glutamic acid with glucose treatment (45µg/g bodyweight glutamic acid and 2g/kg bodyweight glucose) or the control treatment. Regions of interest were drawn to encompass the entire tissue of interest. A) SUV_{MAX} reported in SUV/mm^3 measurements. B) SUV measurements reported in g/ml using same ROIs as SUV_{MAX} measurements. n=3-7, tissues that were not measurable were excluded. "a" denotes a significant difference from control, $p \leq 0.05$.

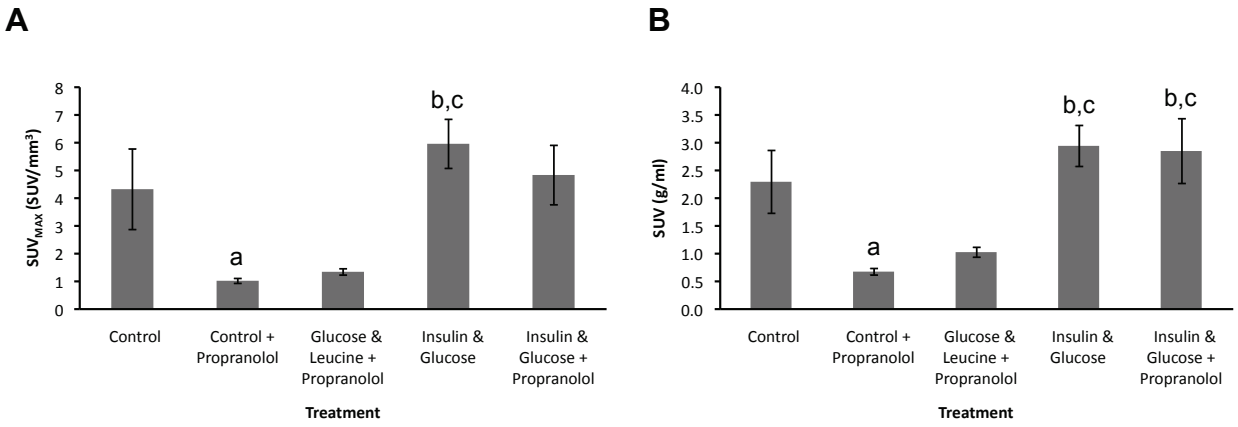

Figure 12: A 10 minute static PET scan was completed 1hr after injection with Control, Glucose & Leucine (2g/kg bodyweight glucose and 40µg/g bodyweight leucine), or Insulin & Glucose treatments (10U/kg bodyweight insulin and 2g/kg bodyweight glucose), either with or without an injection of 150µg/mouse of propranolol 30 minutes prior to treatment injection. Regions of interest were drawn to encompass the entire IBAT. A) SUV_{MAX} reported in SUV/mm^3 measurements. B) SUV measurements reported in g/ml using same ROIs as SUV_{MAX} measurements. n=3-7, tissues that were not measurable were excluded. “a” denotes a significant difference from control, “b” denotes significance from Control + Propranolol and “c” denotes significance from Glucose & Leucine + Propranolol ($p<0.05$ for all).

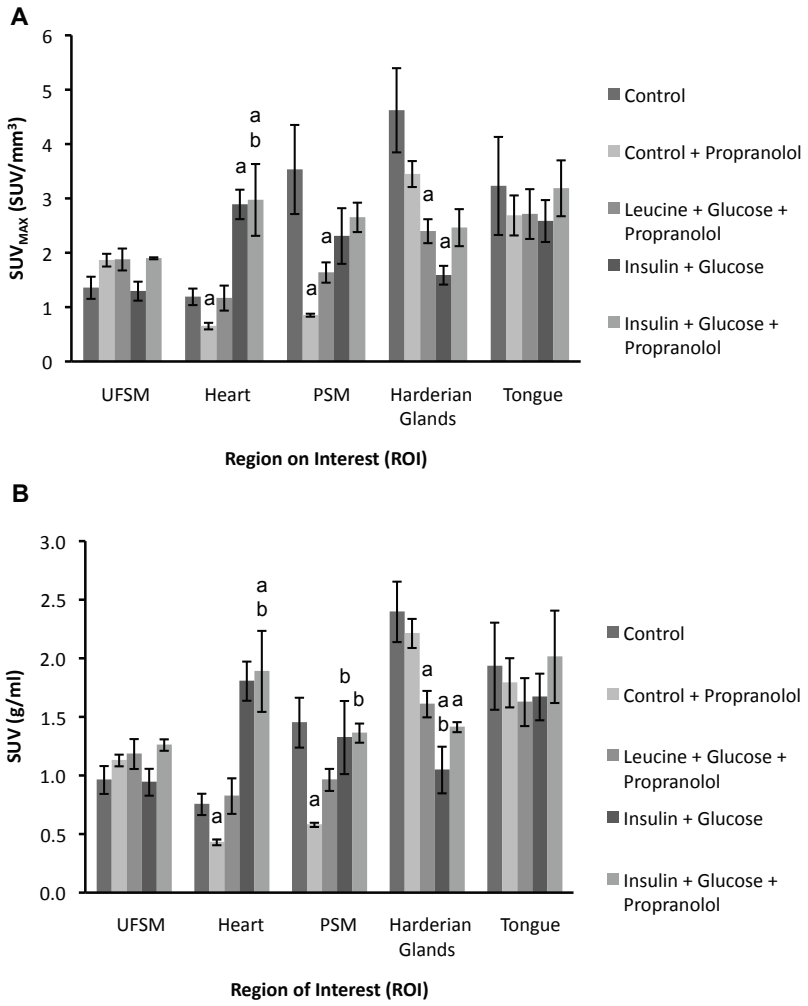

Figure 13: A 10 minute static PET scan was completed 1hr after injection with Control, Glucose & Leucine (2g/kg bodyweight glucose and 40µg/g bodyweight leucine), or Insulin & Glucose (10U/kg bodyweight insulin and 2g/kg bodyweight glucose) treatments, either with or without an injection of 150µg/mouse of propranolol 30 minutes prior to treatment injection. Regions of interest were drawn to encompass the entire tissue of interest. A) SUV_{MAX} reported in SUV/ mm^3 measurements. B) SUV measurements reported in g/ml using same ROIs as SUV_{MAX} measurements. n=3-7, tissues that were not measurable were excluded. “a” denotes a significant difference from control, “b” denotes significance from Control + Propranolol ($p<0.05$ for all).

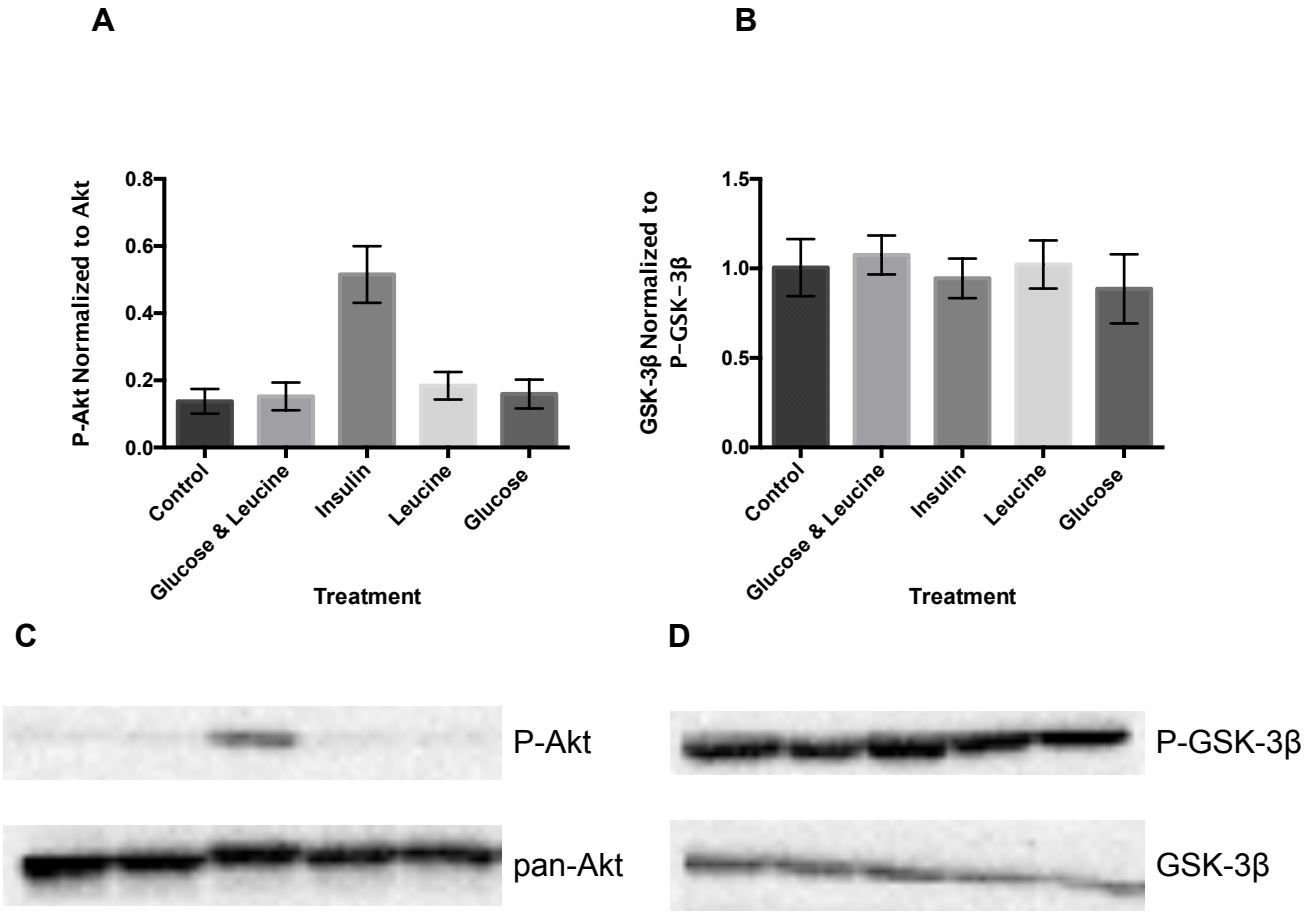

Figure 14: Results from western blots on collected and prepared soleus samples from mice. Treatments Glucose (2g/kg bodyweight), Leucine (40µg/gg bodyweight), Glucose & Leucine (2g/kg bodyweight glucose & 40µg/g leucine), and Insulin (10U/kg bodyweight). 30µg of protein, probed with A) P-Akt antibody, signal quantified and normalized against Akt antibody probed sample pairs. B) GSK-3β antibody, quantified, and normalized against P-GSK-3β antibody probed sample pairs. C) Representative blot of soleus sample with P-Akt and pan-Akt probing. D) Representative blot of soleus sample with GSK-3β and P-GSK-3β.

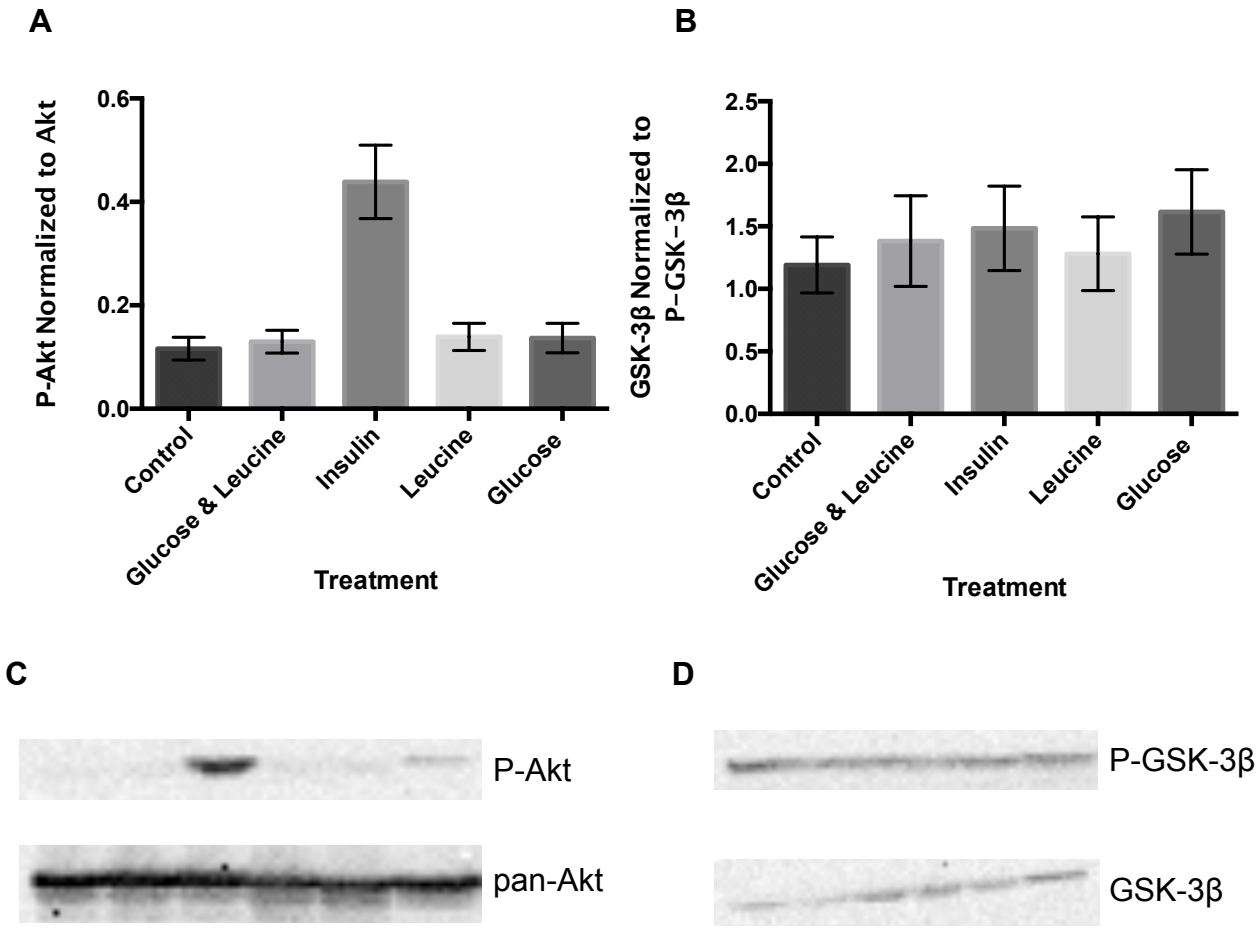

Figure 15: Results from western blots on collected and prepared IBAT samples from mice. Treatments Glucose (2g/kg bodyweight), Leucine (40µg/gg bodyweight), Glucose & Leucine (2g/kg bodyweight glucose & 40µg/g leucine), and Insulin (10U/kg bodyweight). 30µg of protein, probed with A) P-Akt antibody, signal quantified and normalized against Akt antibody probed sample pairs. B) GSK-3β antibody, quantified, and normalized against P-GSK-3β antibody probed sample pairs. C) Representative blot of IBAT sample with P-Akt and pan-Akt probing. D) Representative blot of IBAT sample with GSK-3β and P-GSK-3β.

5. Discussion

In this investigation the efficacy of the leucine as a method of increasing glucose uptake in BAT was analyzed. Literature suggests that leucine plays role in activation of insulin signalling pathways, as well as glucose uptake in skeletal muscle [31]. Similar pathways are responsible for glucose uptake in BAT under certain circumstances, thus it was hypothesized that leucine may act in a similar manner on BAT as it does in skeletal muscle. Leucine is also known to cause increases in circulating insulin when infused, which could lead, indirectly, to stimulation of glucose uptake in tissues such as BAT [32], [33]. This may be one of the methods of action responsible in skeletal muscle as well. It was confirmed through this study that leucine does increase glucose uptake in IBAT when under hyperglycaemic conditions. Following treatment with both glucose, to increase conditions to hyperglycaemia, and leucine, IBAT glucose uptake was significantly increased compared to the control treatment. Interestingly, the results of the present study indicate that adrenergic signalling, and not insulin, are responsible for the leucine-mediated potentiation of glucose uptake in IBAT in hyperglycaemic conditions. To my knowledge, this is the first study to identify the additive effect of glucose and leucine on IBAT glucose metabolism.

5.1 Other Tissues Assessed

Other tissues did not experience significant changes in glucose uptake when leucine was given, with the exception of the harderian glands. It is uncertain why

no increase was observed in the areas that represent skeletal muscle: paraspinal muscles, UFSM, and tongue or in the cardiac tissue. There is evidence that epinephrine can inhibit insulin-stimulated glucose uptake in skeletal muscle. Stress from the imaging experience or epinephrine released due to the temperature being below thermo-neutral for a mouse could cause this [93]. It is also possible that in skeletal muscle and cardiac tissue there was a stealing effect due to the high uptake of ^{18}F-FDG in IBAT. Uptake of ^{18}F-FDG in IBAT during the glucose and glucose and leucine treatments was increased substantially, and could have taken more of the available ^{18}F-FDG leaving the skeletal muscle and cardiac tissue to take up less. Differences in the tongue are likely due to activity of the tongue, such as grooming. Grooming actions use the tongue extensively and would cause changes in uptake due to contraction of the muscle. It is thought that the mice given glucose were actively grooming less, causing the decrease in glucose uptake seen (observations noted during the completion of the study). In the harderian glands a significant decrease in ^{18}F-FDG uptake was measured in treatments with glucose. The exact reason for this is not known, but experimental conditions that affect lubrication of the eyes, which is a main function of the harderian glands, have been shown to alter ^{18}F-FDG uptake in the tissue [94]. Since all other experimental conditions were kept the same between treatments a stable glucose uptake value was expected; it is thought that the increase in competition between ^{18}F-FDG and glucose caused a decrease in ^{18}F-FDG uptake in the harderian glands, similar to what is seen in

tumours [60]. This effect might not be seen in IBAT due to the large increase in total uptake, following leucine and glucose treatment.

5.2 Glucose Treatment

When glucose treatment was given alone, an increase in glucose uptake in IBAT was measured. This increase is likely due to the insulin responsiveness of BAT. The dose of glucose given is based on the amounts given in a glucose tolerance test (GTT) which will elicit a release of endogenous insulin into circulation [95]. Due to the insulin response seen in BAT this increase in insulin would lead to activation of the IR pathway causing the eventual translocation of GLUT 4 to the cell membrane and increase of glucose entering the cell [35]. In both skeletal muscle representative tissues and cardiac tissue, no increase was seen due to glucose treatment. These results are similar to that seen in the treatment with glucose paired with leucine, and is unexpected due to the known insulin responsiveness of these tissues. While the reason for this is unknown, perhaps the magnitude of the insulin response and resulting glucose and ^{18}F-FDG uptake were not sufficiently elevated to offset the competition between ^{18}F-FDG and glucose, resulting in increases in glucose uptake, but not ^{18}F-FDG. This would be due to the increase in non-labeled glucose given through injection diluting the ratio of ^{18}F-FDG to glucose. As mentioned previously this could also be due to a stealing effect, caused by the increase in IBAT ^{18}F-FDG uptake with glucose treatment. This could be potentially tested or solved by giving more ^{18}F-FDG, however the microPET set-up used during the duration of this experiment has a

maximum amount that can be tolerated, that would prevent the completion of this test.

5.3 Glucose and Leucine

One important aspect of the present study involves the finding that leucine alone, did not increase glucose uptake in IBAT, however, when combined with glucose and additive effect was observed in the stimulation of ^{18}F-FDG uptake. This result was unexpected since previous findings have shown that leucine increases circulating insulin [15] and glucose uptake in skeletal muscle [17], [20]. However, it has been reported in literature that leucine treatment can increase insulin sensitivity of tissues [21]. In this case an explanation may be that the magnitude of the insulin increase, even with the increase in insulin sensitivity may not be high enough to over come competition between other tissues in this fasted state. When glucose is added in addition to the leucine the increase in circulating insulin would meet an increase in insulin sensitivity leading to greater uptake. The amount of stimulation caused by the glucose and leucine together would be enough to see a measurable increase in uptake in IBAT and have enough to overcome competition.

5.4 Glutamic Acid

Experiments completed using an alternative amino acid, glutamic acid, did not give the same results as leucine. The glutamic acid treatment was given with the addition of glucose to mimic the successful increase seen by the leucine and

glucose treatment. It was determined that glutamic acid did not have the same enhancement effect on glucose uptake in IBAT when under hyperglycaemic conditions. This is expected since results reported in literature, which infuse glutamic acid did not cause changes in insulin or glucagon levels, which were seen with leucine. This negative result indicates that amino acid action is specific to particular amino acids, versus all amino acids. In other tissues the lack of glucose uptake increase continued. In the harderian gland the decrease in glucose uptake seen in other treatments containing glucose was continued. In skeletal muscle, however, there was decreased ^{18}F-FDG uptake with glutamic acid paired with a glucose injection in some of the regions examined (UFSM and tongue).

5.5 Signalling Pathway

In order to gather information related to the signalling pathway responsible for the increase in glucose uptake resulting from the treatment with leucine and glucose, tissues were collected after treatments and analyzed. IBAT and soleus muscle were collected following treatments and western blotting performed and probed with P-Akt/pan-Akt and P-GSK-3β/GSK-3β. Knowing that the insulin stimulated pathway leads to the phosphorylation of Akt (activations) and GSK-3β (inhibition) and that increased beta adrenergic activity only leads to the inhibition of GSK-3β (increased phosphorylation) conclusions about treatment activation can be drawn. In IBAT there were no significant differences in P-Akt levels except between insulin treatment and all other treatments. There was a significant

increase in the phosphorylation of Akt after insulin treatment. Non-significant increases in p-Akt/pan-Akt of 17%, 16%, and 11% were observed for glucose and leucine, leucine, and glucose treatments, respectively. p-GSK-3β/GSK-3β ratio in IBAT were not significantly different for any treatment. Non-significant increases in p-GSK-3β/GSK-3β of 7%, 30%, and 15% were observed for glucose and leucine, leucine, and glucose treatments, respectively. One possible explanation is that the effect on signalling in the tissues due to these treatments, was below detection limits using the method of western blot and ECL used. Insulin was the only treatment able to cause measurable significant increases in P-Akt signalling.

In addition to quantifying cell signalling, the use of a beta blocker prior to imaging was investigated. The beta blocker propranolol has been shown to have a near complete blocking effect on beta receptor action in mice. Propranolol is a non-specific beta blocker that acts on all beta receptors [27]. Since the action of non-shivering thermogenesis occurs through a beta adrenergic receptor, propranolol would nearly abolish all action through this pathway. The method of action of the leucine treatment is uncertain and could have beta-adrenergic involvement. By blocking this method of activation it can be determined if another pathway of action, such as an insulin related action, is involved. If a increase in glucose uptake in IBAT remains after pretreatment, then another method of activation is involved. Pretreatment with propranolol did prevent a significant increase in ^{18}F-FDG uptake in response to leucine and glucose. This finding does indicate the

involvement of beta adrenergic signalling in the stimulation of leucine and glucose-mediated ^{18}F-FDG uptake. However, a non-significant increase of 41% was still observed. Therefore, it is possible that the method of action is not completely through a beta-adrenergic pathway, and the role of insulin signalling should not be ruled out. To test if this pathway is still active after pretreatment with propranolol, a near maximal dose of insulin was given, both with and without propranolol. Insulin did increase ^{18}F-FDG uptake in IBAT, with no significant difference observed with propranolol pretreatment before insulin. This indicates that this pathway is not inhibited due to the use of propranolol. The slight increase in glucose uptake in the IBAT between glucose with leucine and control, both with propranolol pretreatment, might then be due to activation through a small increase in circulating insulin caused by leucine injection. It should be noted however that this slight increase could be caused by a different pathway of activation, such as a CBL related pathway acting on the IR through a PI3K independent pathway. This pathway, however, is suggested to be downstream of IRS-1, requiring activation to initiate eventual GLUT4 translocation [95]. This would mean that insulin would be required for either of these methods of activation. Suggesting that an increase of glucose uptake in IBAT would come from an insulin related pathway. Since the majority of basal glucose uptake (non-stimulated) is blocked with propranolol, the major pathway of activation is β-adrenergic, but it cannot be said if this is caused by the treatment or by activation caused by non-shivering thermogenesis. This pathway could be active since mice are thermo-neutral between 30°C and 34°C and the housing and

experiment conditions was 22°C ± 3°C [60]. therefore the BAT was thermogenically active in our studies and all of the treatment effects were in the presence of beta-adrenergically activated tissue. It is possible that when this main form of activation is blocked the treatment effect of glucose and leucine may be less. It is also possible that the main form of activation caused by the treatment is β-adrenergic. Further signalling studies with either insulin action antagonists and imaging or collected tissues would need to be performed to determine the method of action.

In skeletal muscle there were no significant differences seen between the groups, but a slight increase in treatments that had pretreatment with propranolol. Literature suggests that beta-adrenergic activity on skeletal muscle decreases the amount of GLUT 4 in the muscle [96]. If the propranolol blocked beta-adrenergic action in the muscle, it is possible that membrane GLUT 4 content could increased. There is however little data on beta-blocker use and GLUT 4 response and more information is needed to formulate a better picture of the effects. However, it has also been reported that the use of beta-blockers can reduce peripheral blood flow, which can limit glucose disposal into skeletal muscle [97]. This was not seen in the present study, but it is also suggested in literature that the reduced peripheral blood flow during initial use of a beta-blocker is offset by a rise in vascular resistance [98]. Since the use of propranolol is not long term these affects may have been offset for these experiments. In cardiac tissue propranolol lowered glucose uptake, which is expected due to beta

receptor antagonists lowering heart rate, contractility, conduction velocity, and relaxation rate [99]. The leucine and glucose injections seemed to negate the effects of the beta-blocker seen with the pretreatment of propranolol. This could be due to increases in circulating insulin caused by the treatment, since cardiac tissue is highly insulin responsive [100]. The reason this increase was not seen with previous treatments could be due to the activity from the adrenergic receptors masking the response from the slight circulating insulin increase. Like seen previously glucose uptake in the harderian gland was decreased with treatments containing glucose; propranolol seemed to have no effect on this tissue.

5.6 The Use of PET Imaging for Quantifying Glucose Uptake in Tissues

These results indicate that PET imaging is a good candidate for assessing tissue specific glucose uptake in some organs. It is able to detect differences in BAT glucose uptake due to various treatments, which is useful for future BAT work as it continues to be of interest for metabolic disease prevention and treatment. The benefit of PET is the non-invasive nature of this testing as well as the speed of measurement. Considering most tissue specific glucose measurements require dissection it is not viable in human studies, PET opens the opportunity for clinical work in this field. These results also indicate that leucine has good potential to help activate BAT in hyperglycaemic conditions which has promise to aid in treating insulin resistance and metabolic disease.

Another application that can make use of PET for tissue specific glucose uptake measurements is cardiac tissue. Current methods of testing heart tissue specific insulin resistance are done through cell culture models or perfusion models [84], [101]. These methods are not testable in live individuals and are done ex vivo. Developing testing practices that can be completed in live patients could have positive impacts on mechanism of action, diagnosis, and prevention for at risk individuals. This development is important since cardiovascular disease and stroke are the number one cause of death in individuals, especially those with diabetes. In this study differences in heart were not seen with the treatments given, however it is suspected this is related to other causes, not the inability of PET to distinguish differences. This is because in preliminary imaging and during testing with insulin, differences where seen with insulin treatment as well as varying fasting conditions.

6. Conclusion

Hyperglycaemia is a prominent clinical outcome in obese and T2D populations [70]. Using dietary methods to aid in controlling these glucose levels as well as to potentially prevent the development of T2D could be an important key in a growing epidemic. Current methods focus on drug treatments as well as a controlled diet and exercise regime, however the latter can often be difficult to put into practice. The use of a dietary supplement has the benefit of being easy to implement. The amino acid leucine, shows to be a promising candidate at

increasing glucose uptake as well as energy expenditure, through BAT activation, in a hyperglycaemic state. PET imaging of glucose uptake in IBAT following treatment shows increases in glucose uptake, which is correlated to activation of the tissue.

7. Literature Cited

[1] Statistics Canada, “Health indicator profile, annual estimates, by age group and sex, Canada, provinces, territories, health regions (2013 boundaries) and peer groups, occasional.” CANSIM, 16-Jun-2015.

[2] David C.W. Lau, James D. Douketis, Katherine M. Morrison, Irene M. Hramiak, Arya M. Sharma, and Ehud Ur, “2006 Canadian clinical practice guidelines on the management and prevention of obesity in adults and children [summary],” *CMAJ*, vol. 176, no. 8, pp. S1–13, Apr. 2007.

[3] W. D. van Marken Lichtenbelt, J. W. Vanhommerig, N. M. Smulders, J. M. A. F. L. Drossaerts, G. J. Kemerink, N. D. Bouvy, P. Schrauwen, and G. J. J. Teule, “Cold-activated brown adipose tissue in healthy men,” *N. Engl. J. Med.*, vol. 360, no. 15, pp. 1500–1508, Apr. 2009.

[4] A. M. Cypess, S. Lehman, G. Williams, I. Tal, D. Rodman, A. B. Goldfine, F. C. Kuo, E. L. Palmer, Y.-H. Tseng, A. Doria, G. M. Kolodny, and C. R. Kahn, “Identification and importance of brown adipose tissue in adult humans,” *N. Engl. J. Med.*, vol. 360, no. 15, pp. 1509–1517, Apr. 2009.

[5] K. A. Virtanen, M. E. Lidell, J. Orava, M. Heglind, R. Westergren, T. Niemi, M. Taittonen, J. Laine, N.-J. Savisto, S. Enerbäck, and P. Nuutila, “Functional brown adipose tissue in healthy adults,” *N. Engl. J. Med.*, vol. 360, no. 15, pp. 1518–1525, Apr. 2009.

[6] M. Saito, Y. Okamatsu-Ogura, M. Matsushita, K. Watanabe, T. Yoneshiro, J. Nio-Kobayashi, T. Iwanaga, M. Miyagawa, T. Kameya, K. Nakada, Y. Kawai, and M. Tsujisaki, “High incidence of metabolically active brown adipose tissue in healthy adult humans: effects of cold exposure and adiposity,” *Diabetes*, vol. 58, no. 7, pp. 1526–1531, Jul. 2009.

[7] M. J. Vosselman, B. Brans, A. A. J. J. van der Lans, R. Wierts, M. A. van Baak, F. M. Mottaghy, P. Schrauwen, and W. D. van Marken Lichtenbelt, “Brown adipose tissue activity after a high-calorie meal in humans,” *Am. J. Clin. Nutr.*, vol. 98, no. 1, pp. 57–64, Jul. 2013.

[8] D. Richard, A. C. Carpentier, G. Doré, V. Ouellet, and F. Picard, “Determinants of brown adipocyte development and thermogenesis,” Int J Obes (Lond), vol. 34 Suppl 2, pp. S59–66, Dec. 2010.

[9] J. Villarroya, R. Cereijo, and F. Villarroya, “An endocrine role for brown adipose tissue?,” *Am. J. Physiol. Endocrinol. Metab.*, vol. 305, no. 5, pp. E567–572, Sep. 2013.

[10] D. K. Layman and D. A. Walker, “Potential importance of leucine in treatment of obesity and the metabolic syndrome,” *J. Nutr.*, vol. 136, no. 1 Suppl, p. 319S–23S, Jan. 2006.

[11] L. McAllan, P. D. Cotter, H. M. Roche, R. Korpela, and K. N. Nilaweera, “Impact of leucine on energy balance,” *J. Physiol. Biochem.*, vol. 69, no. 1, pp. 155–163, Mar. 2013.

[12] M. H. Stipanuk, “Leucine and protein synthesis: mTOR and beyond,” *Nutr. Rev.*, vol. 65, no. 3, pp. 122–129, Mar. 2007.

[13] C. J. Lynch, B. J. Patson, J. Anthony, A. Vaval, L. S. Jefferson, and T. C. Vary, “Leucine is a direct-acting nutrient signal that regulates protein synthesis in adipose tissue,” *Am. J. Physiol. Endocrinol. Metab.*, vol. 283, no. 3, pp. E503–513, Sep. 2002.
[14] O. N. Ulutin and G. Cizmeci, “Alteration of prostanoids in atherosclerosis,” Semin. Thromb. Hemost., vol. 11, no. 4, pp. 362–366, Oct. 1985.
[15] T. Kuhara, S. Ikeda, A. Ohneda, and Y. Sasaki, “Effects of intravenous infusion of 17 amino acids on the secretion of GH, glucagon, and insulin in sheep,” Am. J. Physiol., vol. 260, no. 1 Pt 1, pp. E21–26, Jan. 1991.
[16] P. J. Garlick, “The role of leucine in the regulation of protein metabolism,” J. Nutr., vol. 135, no. 6 Suppl, p. 1553S–6S, Jun. 2005.
[17] P. J. Garlick and I. Grant, “Amino acid infusion increases the sensitivity of muscle protein synthesis in vivo to insulin. Effect of branched-chain amino acids,” Biochem. J., vol. 254, no. 2, pp. 579–584, Sep. 1988.
[18] K. Peyrollier, E. Hajduch, A. S. Blair, R. Hyde, and H. S. Hundal, “L-leucine availability regulates phosphatidylinositol 3-kinase, p70 S6 kinase and glycogen synthase kinase-3 activity in L6 muscle cells: evidence for the involvement of the mammalian target of rapamycin (mTOR) pathway in the L-leucine-induced up-regulation of system A amino acid transport,” Biochem. J., vol. 350 Pt 2, pp. 361–368, Sep. 2000.
[19] J. C. Anthony, C. H. Lang, S. J. Crozier, T. G. Anthony, D. A. MacLean, S. R. Kimball, and L. S. Jefferson, “Contribution of insulin to the translational control of protein synthesis in skeletal muscle by leucine,” Am. J. Physiol. Endocrinol. Metab., vol. 282, no. 5, pp. E1092–1101, May 2002.
[20] S. Nishitani, T. Matsumura, S. Fujitani, I. Sonaka, Y. Miura, and K. Yagasaki, “Leucine promotes glucose uptake in skeletal muscles of rats,” Biochem. Biophys. Res. Commun., vol. 299, no. 5, pp. 693–696, Dec. 2002.
[21] Y. Zhang, K. Guo, R. E. LeBlanc, D. Loh, G. J. Schwartz, and Y.-H. Yu, “Increasing dietary leucine intake reduces diet-induced obesity and improves glucose and cholesterol metabolism in mice via multimechanisms,” Diabetes, vol. 56, no. 6, pp. 1647–1654, Jun. 2007.
[22] A. A. J. J. van der Lans, J. Hoeks, B. Brans, G. H. E. J. Vijgen, M. G. W. Visser, M. J. Vosselman, J. Hansen, J. A. Jörgensen, J. Wu, F. M. Mottaghy, P. Schrauwen, and W. D. van Marken Lichtenbelt, “Cold acclimation recruits human brown fat and increases nonshivering thermogenesis,” Journal of Clinical Investigation, vol. 123, no. 8, pp. 3395–3403, Aug. 2013.
[23] P. Iozzo, “Metabolic imaging in obesity: underlying mechanisms and consequences in the whole body,” Ann. N. Y. Acad. Sci., vol. 1353, pp. 21–40, Sep. 2015.
[24] K. I. Stanford, R. J. W. Middelbeek, K. L. Townsend, D. An, E. B. Nygaard, K. M. Hitchcox, K. R. Markan, K. Nakano, M. F. Hirshman, Y.-H. Tseng, and L. J. Goodyear, “Brown adipose tissue regulates glucose homeostasis and insulin sensitivity,” J. Clin. Invest., vol. 123, no. 1, pp. 215–223, Jan. 2013.
[25] C. S. Tam, V. Lecoultre, and E. Ravussin, “Brown adipose tissue: mechanisms and potential therapeutic targets,” Circulation, vol. 125, no. 22, pp. 2782–2791, Jun. 2012.

[26] Y. Shimizu, H. Nikami, and M. Saito, “Sympathetic activation of glucose utilization in brown adipose tissue in rats,” J. Biochem., vol. 110, no. 5, pp. 688–692, Nov. 1991.
[27] M. R. Mirbolooki, C. C. Constantinescu, M.-L. Pan, and J. Mukherjee, “Quantitative assessment of brown adipose tissue metabolic activity and volume using 18F-FDG PET/CT and β3-adrenergic receptor activation,” *EJNMMI Res.*, vol. 1, no. 1, p. 30, 2011.
[28] P. Felig and J. Wahren, “Influence of Endogenous Insulin Secretion on Splanchnic Glucose and Amino Acid Metabolism in Man,” *J. Clin. Invest.*, vol. 50, no. 8, pp. 1702–1711, Aug. 1971.
[29] R. A. DeFronzo, J. D. Tobin, and R. Andres, “Glucose clamp technique: a method for quantifying insulin secretion and resistance,” *Am. J. Physiol.*, vol. 237, no. 3, pp. E214–223, Sep. 1979.
[30] D. K. Andersen, D. Elahi, J. C. Brown, J. D. Tobin, and R. Andres, “Oral glucose augmentation of insulin secretion. Interactions of gastric inhibitory polypeptide with ambient glucose and insulin levels,” *J. Clin. Invest.*, vol. 62, no. 1, pp. 152–161, Jul. 1978.
[31] A. Suryawan, R. A. Orellana, M. L. Fiorotto, and T. A. Davis, “Triennial Growth Symposium: leucine acts as a nutrient signal to stimulate protein synthesis in neonatal pigs,” *J. Anim. Sci.*, vol. 89, no. 7, pp. 2004–2016, Jul. 2011.
[32] P. J. Garlick and I. Grant, “Amino acid infusion increases the sensitivity of muscle protein synthesis in vivo to insulin. Effect of branched-chain amino acids,” *Biochem. J.*, vol. 254, no. 2, pp. 579–584, Sep. 1988.
[33] T. Kuhara, S. Ikeda, A. Ohneda, and Y. Sasaki, “Effects of intravenous infusion of 17 amino acids on the secretion of GH, glucagon, and insulin in sheep,” *Am. J. Physiol.*, vol. 260, no. 1 Pt 1, pp. E21–26, Jan. 1991.
[34] P. J. Garlick and I. Grant, “Amino acid infusion increases the sensitivity of muscle protein synthesis in vivo to insulin. Effect of branched-chain amino acids,” Biochem. J., vol. 254, no. 2, pp. 579–584, Sep. 1988.
[35] B. Cannon, “Brown Adipose Tissue: Function and Physiological Significance,” *Physiol. Rev.*, vol. 84, no. 1, pp. 277–359, Jan. 2004.
[36] Y. Zhu, R. O. Pereira, B. T. O’Neill, C. Riehle, O. Ilkun, A. R. Wende, T. A. Rawlings, Y. C. Zhang, Q. Zhang, A. Klip, I. Shiojima, K. Walsh, and E. D. Abel, “Cardiac PI3K-Akt impairs insulin-stimulated glucose uptake independent of mTORC1 and GLUT4 translocation,” *Mol. Endocrinol. Baltim. Md*, vol. 27, no. 1, pp. 172–184, Jan. 2013.
[37] N. Houstis, E. D. Rosen, and E. S. Lander, “Reactive oxygen species have a causal role in multiple forms of insulin resistance,” *Nature*, vol. 440, no. 7086, pp. 944–948, Apr. 2006.
[38] M. Larance, G. Ramm, and D. E. James, “The GLUT4 code,” *Mol. Endocrinol. Baltim. Md*, vol. 22, no. 2, pp. 226–233, Feb. 2008.
[39] L. Boutens and R. Stienstra, “Adipose tissue macrophages: going off track during obesity,” Diabetologia, vol. 59, no. 5, pp. 879–894, May 2016.

[40] C. Roberts-Toler, B. T. O'Neill, and A. M. Cypess, "Diet-induced obesity causes insulin resistance in mouse brown adipose tissue," Obesity (Silver Spring), vol. 23, no. 9, pp. 1765–1770, Sep. 2015.
[41] D. L. Bailey, Ed., *Positron emission tomography: basic sciences*. New York: Springer, 2005.
[42] A. Shukla and U. Kumar, "Positron emission tomography: An overview," *J. Med. Phys.*, vol. 31, no. 1, p. 13, 2006.
[43] M. E. Phelps, E. J. Hoffman, S. C. Huang, and M. M. Ter-Pogossian, "Effect of positron range on spatial resolution," *J. Nucl. Med. Off. Publ. Soc. Nucl. Med.*, vol. 16, no. 7, pp. 649–652, Jul. 1975.
[44] C. S. Levin and E. J. Hoffman, "Calculation of positron range and its effect on the fundamental limit of positron emission tomography system spatial resolution," *Phys. Med. Biol.*, vol. 44, no. 3, pp. 781–799, Mar. 1999.
[45] T. K. Lewellen, "Recent developments in PET detector technology," *Phys. Med. Biol.*, vol. 53, no. 17, pp. R287–R317, Sep. 2008.
[46] E. Miele, G. Spinelli, F. Tomao, A. Zullo, F. De Marinis, G. Pasciuti, L. Rossi, F. Zoratto, and S. Tomao, "Positron Emission Tomography (PET) radiotracers in oncology – utility of 18F-Fluoro-deoxy-glucose (FDG)-PET in the management of patients with non-small-cell lung cancer (NSCLC)," *J. Exp. Clin. Cancer Res.*, vol. 27, no. 1, p. 52, 2008.
[47] G. L. Kellett, E. Brot-Laroche, O. J. Mace, and A. Leturque, "Sugar Absorption in the Intestine: The Role of GLUT2," *Annu. Rev. Nutr.*, vol. 28, no. 1, pp. 35–54, Aug. 2008.
[48] K. M. Eny, T. M. S. Wolever, B. Fontaine-Bisson, and A. El-Sohemy, "Genetic variant in the glucose transporter type 2 is associated with higher intakes of sugars in two distinct populations," *Physiol. Genomics*, vol. 33, no. 3, pp. 355–360, May 2008.
[49] T. A. D. Smith, "The rate-limiting step for tumor [18F]fluoro-2-deoxy-D-glucose (FDG) incorporation," *Nucl. Med. Biol.*, vol. 28, no. 1, pp. 1–4, Jan. 2001.
[50] K. Kubota, H. Watanabe, Y. Murata, M. Yukihiro, K. Ito, M. Morooka, R. Minamimoto, A. Hori, and H. Shibuya, "Effects of blood glucose level on FDG uptake by liver: a FDG-PET/CT study," Nucl. Med. Biol., vol. 38, no. 3, pp. 347–351, Apr. 2011.
[51] E. van Schaftingen and I. Gerin, "The glucose-6-phosphatase system," *Biochem. J.*, vol. 362, no. Pt 3, pp. 513–532, Mar. 2002.
[52] A. R. Thiam, R. V. Farese Jr, and T. C. Walther, "The biophysics and cell biology of lipid droplets," *Nat. Rev. Mol. Cell Biol.*, vol. 14, no. 12, pp. 775–786, Nov. 2013.
[53] P. Wang, E. Mariman, J. Renes, and J. Keijer, "The secretory function of adipocytes in the physiology of white adipose tissue," *J. Cell. Physiol.*, vol. 216, no. 1, pp. 3–13, Jul. 2008.
[54] C. Pagano, A. Calcagno, L. Giacomelli, A. Poletti, V. Macchi, R. Vettor, R. De Caro, and G. Federspil, "Molecular and morphometric description of adipose tissue during weight changes: a quantitative tool for assessment of tissue texture," *Int. J. Mol. Med.*, vol. 14, no. 5, pp. 897–902, Nov. 2004.

[55] H. Terada, “Uncouplers of oxidative phosphorylation.,” *Environ. Health Perspect.*, vol. 87, pp. 213–218, Jul. 1990.
[56] D. Richard and F. Picard, “Brown fat biology and thermogenesis,” Front Biosci (Landmark Ed), vol. 16, pp. 1233–1260, 2011.
[57] A. Fedorenko, P. V. Lishko, and Y. Kirichok, “Mechanism of fatty-acid-dependent UCP1 uncoupling in brown fat mitochondria,” *Cell*, vol. 151, no. 2, pp. 400–413, Oct. 2012.
[58] V. Ouellet, S. M. Labbé, D. P. Blondin, S. Phoenix, B. Guérin, F. Haman, E. E. Turcotte, D. Richard, and A. C. Carpentier, “Brown adipose tissue oxidative metabolism contributes to energy expenditure during acute cold exposure in humans,” J. Clin. Invest., vol. 122, no. 2, pp. 545–552, Feb. 2012.
[59] N. J. Rothwell and M. J. Stock, “A role for brown adipose tissue in diet-induced thermogenesis,” Nature, vol. 281, no. 5726, pp. 31–35, Sep. 1979.
[60] B. J. Fueger, J. Czernin, I. Hildebrandt, C. Tran, B. S. Halpern, D. Stout, M. E. Phelps, and W. A. Weber, “Impact of animal handling on the results of 18F-FDG PET studies in mice,” J. Nucl. Med., vol. 47, no. 6, pp. 999–1006, Jun. 2006.
[61] J. R. Lupien, Z. Glick, M. Saito, and G. A. Bray, “Guanosine diphosphate binding to brown adipose tissue mitochondria is increased after single meal,” Am. J. Physiol., vol. 249, no. 6 Pt 2, pp. R694–698, Dec. 1985.
[62] Z. Glick, S. Y. Wu, J. Lupien, R. Reggio, G. A. Bray, and D. A. Fisher, “Meal-induced brown fat thermogenesis and thyroid hormone metabolism in rats,” Am. J. Physiol., vol. 249, no. 5 Pt 1, pp. E519–524, Nov. 1985.
[63] Z. Glick, R. J. Teague, and G. A. Bray, “Brown adipose tissue: thermic response increased by a single low protein, high carbohydrate meal,” Science, vol. 213, no. 4512, pp. 1125–1127, Sep. 1981.
[64] Z. Glick and W. J. Raum, “Norepinephrine turnover in brown adipose tissue is stimulated by a single meal,” Am. J. Physiol., vol. 251, no. 1 Pt 2, pp. R13–17, Jul. 1986.
[65] C. Bing, S. T. Russell, E. E. Beckett, P. Collins, S. Taylor, R. Barraclough, M. J. Tisdale, and G. Williams, “Expression of uncoupling proteins-1, -2 and -3 mRNA is induced by an adenocarcinoma-derived lipid-mobilizing factor,” Br. J. Cancer, vol. 86, no. 4, pp. 612–618, Feb. 2002.
[66] B. Cannon and J. Nedergaard, “Nonshivering thermogenesis and its adequate measurement in metabolic studies,” *J. Exp. Biol.*, vol. 214, no. Pt 2, pp. 242–253, Jan. 2011.
[67] J. Boucher, M. A. Mori, K. Y. Lee, G. Smyth, C. W. Liew, Y. Macotela, M. Rourk, M. Bluher, S. J. Russell, and C. R. Kahn, “Impaired thermogenesis and adipose tissue development in mice with fat-specific disruption of insulin and IGF-1 signalling,” *Nat. Commun.*, vol. 3, p. 902, 2012.
[68] B. B. Lowell, V. S-Susulic, A. Hamann, J. A. Lawitts, J. Himms-Hagen, B. B. Boyer, L. P. Kozak, and J. S. Flier, “Development of obesity in transgenic mice after genetic ablation of brown adipose tissue,” Nature, vol. 366, no. 6457, pp. 740–742, Dec. 1993.

[69] A. Hamann, J. S. Flier, and B. B. Lowell, “Decreased brown fat markedly enhances susceptibility to diet-induced obesity, diabetes, and hyperlipidemia,” Endocrinology, vol. 137, no. 1, pp. 21–29, Jan. 1996.
[70] J. Baynes and M. H. Dominiczak, Medical biochemistry, 3. ed. Edinburgh: Mosby, 2009.
[71] T. W. Batts, E. E. Spangenburg, C. W. Ward, S. J. Lees, and J. H. Williams, “Effects of acute epinephrine treatment on skeletal muscle Sarcoplasmic Reticulum Ca2+ ATPase.,” Basic Appl. Myol., vol. 17, pp. 229–235, 2007.
[72] T. W. Batts, S. J. Lees, and J. H. Williams, “Combined effects of exercise and fasting on skeletal muscle glycogen and sarcoplasmic reticulum function.,” Basic Appl. Myol., vol. 19, pp. 247–252, 2009.
[73] L. Ramalingam, E. Oh, and D. C. Thurmond, “Novel roles for insulin receptor (IR) in adipocytes and skeletal muscle cells via new and unexpected substrates,” Cellular and Molecular Life Sciences, vol. 70, no. 16, pp. 2815–2834, Aug. 2013.
[74] P. Iozzo, P. Chareonthaitawee, D. Dutka, D. J. Betteridge, E. Ferrannini, and P. G. Camici, “Independent association of type 2 diabetes and coronary artery disease with myocardial insulin resistance,” *Diabetes*, vol. 51, no. 10, pp. 3020–3024, Oct. 2002.
[75] R. M. Witteles, W. H. W. Tang, A. H. Jamali, J. W. Chu, G. M. Reaven, and M. B. Fowler, “Insulin resistance in idiopathic dilated cardiomyopathy: a possible etiologic link,” *J. Am. Coll. Cardiol.*, vol. 44, no. 1, pp. 78–81, Jul. 2004.
[76] Ronald Aubert, *Diabetes in America*, 2nd ed. DIANE Publishing, 1995.
[77] Earl S. Ford, “Risks for All-Cause Mortality, Cardiovascular Disease, and Diabetes Associated With the Metabolic Syndrome,” *Diabetes Care*, vol. 28, no. 7, pp. 1769–1778, Jul. 2005.
[78] Zachary T. Bloomgarden, “Cardiovascular Disease and Diabetes,” *Diabetes Care*, vol. 26, no. 1, pp. 230–237, Jan. 2003.
[79] M. P. Stern, “Diabetes and cardiovascular disease. The ‘common soil’ hypothesis,” Diabetes, vol. 44, no. 4, pp. 369–374, Apr. 1995.
[80] G. Paternostro, D. Pagano, T. Gnecchi-Ruscone, R. S. Bonser, and P. G. Camici, “Insulin resistance in patients with cardiac hypertrophy,” *Cardiovasc. Res.*, vol. 42, no. 1, pp. 246–253, Apr. 1999.
[81] M. Taylor, T. R. Wallhaus, T. R. Degrado, D. C. Russell, P. Stanko, R. J. Nickles, and C. K. Stone, “An evaluation of myocardial fatty acid and glucose uptake using PET with [18F]fluoro-6-thia-heptadecanoic acid and [18F]FDG in Patients with Congestive Heart Failure,” *J. Nucl. Med. Off. Publ. Soc. Nucl. Med.*, vol. 42, no. 1, pp. 55–62, Jan. 2001.
[82] G. Paternostro, P. G. Camici, A. A. Lammerstma, N. Marinho, R. R. Baliga, J. S. Kooner, G. K. Radda, and E. Ferrannini, “Cardiac and skeletal muscle insulin resistance in patients with coronary heart disease. A study with positron emission tomography,” *J. Clin. Invest.*, vol. 98, no. 9, pp. 2094–2099, Nov. 1996.

[83] M. Skrzypiec-Spring, B. Grotthus, A. Szelag, and R. Schulz, “Isolated heart perfusion according to Langendorff---still viable in the new millennium,” *J. Pharmacol. Toxicol. Methods*, vol. 55, no. 2, pp. 113–126, Apr. 2007.
[84] D. Gross, *Animal Models in Cardiovascular Research*. New York, NY: Springer US, 2009.
[85] S. Dhein, F. W. Mohr, and M. Delmar, Eds., *Practical methods in cardiovascular research*. Berlin ; New York: Springer, 2005.
[86] W. E. Louch, K. A. Sheehan, and B. M. Wolska, “Methods in cardiomyocyte isolation, culture, and gene transfer,” *J. Mol. Cell. Cardiol.*, vol. 51, no. 3, pp. 288–298, Sep. 2011.
[87] J. S. Mitcheson, J. C. Hancox, and A. J. Levi, “Cultured adult cardiac myocytes: future applications, culture methods, morphological and electrophysiological properties,” *Cardiovasc. Res.*, vol. 39, no. 2, pp. 280–300, Aug. 1998.
[88] V. Salem, C. Izzi-Engbeaya, C. Coello, D. B. Thomas, E. S. Chambers, A. N. Comninos, A. Buckley, Z. Win, A. Al-Nahhas, E. A. Rabiner, R. N. Gunn, H. Budge, M. E. Symonds, S. R. Bloom, T. M. Tan, and W. S. Dhillo, “Glucagon increases energy expenditure independently of brown adipose tissue activation in humans,” Diabetes Obes Metab, vol. 18, no. 1, pp. 72–81, Jan. 2016.
[89] K. Tanaka, T. Kawano, A. Nakamura, H. Nazari, S. Kawahito, S. Oshita, A. Takahashi, and Y. Nakaya, “Isoflurane activates sarcolemmal adenosine triphosphate-sensitive potassium channels in vascular smooth muscle cells: a role for protein kinase A,” Anesthesiology, vol. 106, no. 5, pp. 984–991, May 2007.
[90] B. Jespersen, N. R. Tykocki, S. W. Watts, and P. J. Cobbett, “Measurement of Smooth Muscle Function in the Isolated Tissue Bath-applications to Pharmacology Research,” Journal of Visualized Experiments, no. 95, Jan. 2015.
[91] M. C. Kreissl, D. B. Stout, K.-P. Wong, H.-M. Wu, E. Caglayan, W. Ladno, X. Zhang, J. O. Prior, C. Reiners, S.-C. Huang, and H. R. Schelbert, “Influence of dietary state and insulin on myocardial, skeletal muscle and brain [18F]-fluorodeoxyglucose kinetics in mice,” EJNMMI Research, vol. 1, no. 1, p. 8, 2011.
[92] I. Yokoyama, Y. Inoue, T. Moritan, K. Ohtomo, and R. Nagai, “Simple quantification of skeletal muscle glucose utilization by static 18F-FDG PET,” J. Nucl. Med., vol. 44, no. 10, pp. 1592–1598, Oct. 2003.
[93] J. L. Chiasson, H. Shikama, D. T. Chu, and J. H. Exton, “Inhibitory effect of epinephrine on insulin-stimulated glucose uptake by rat skeletal muscle,” J. Clin. Invest., vol. 68, no. 3, pp. 706–713, Sep. 1981.
[94] M. Kim et al., “Effect of Harderian adenectomy on the statistical analyses of mouse brain imaging using positron emission tomography,” Journal of Veterinary Science, vol. 15, no. 1, p. 157, 2014.
[95] A. Miura, M. P. Sajan, M. L. Standaert, G. Bandyopadhyay, C. R. Kahn, and R. V. Farese, “Insulin substrates 1 and 2 are corequired for activation of atypical protein kinase C and Cbl-dependent phosphatidylinositol 3-kinase

during insulin action in immortalized brown adipocytes," Biochemistry, vol. 43, no. 49, pp. 15503–15509, Dec. 2004.
[96] G. S. Lynch and J. G. Ryall, "Role of beta-adrenoceptor signaling in skeletal muscle: implications for muscle wasting and disease," Physiol. Rev., vol. 88, no. 2, pp. 729–767, Apr. 2008.
[97] J. E. Ayala et al., "Standard operating procedures for describing and performing metabolic tests of glucose homeostasis in mice," Dis Model Mech, vol. 3, no. 9–10, pp. 525–534, Oct. 2010.
[98] A. J. Man in't Veld, A. H. Van den Meiracker, and M. A. Schalekamp, "Do beta-blockers really increase peripheral vascular resistance? Review of the literature and new observations under basal conditions," Am. J. Hypertens., vol. 1, no. 1, pp. 91–96, Jan. 1988.
[99] D. F. Blackburn and T. W. Wilson, "Antihypertensive medications and blood sugar: Theories and implications," Canadian Journal of Cardiology, vol. 22, no. 3, pp. 229–233, Mar. 2006.
[100] E. F. du Toit and D. G., "Myocardial Insulin Resistance: An Overview of Its Causes, Effects, and Potential Therapy," in Insulin Resistance, S. Arora, Ed. InTech, 2012.
[101] S. L. Jacobson and H. M. Piper, "Cell cultures of adult cardiomyocytes as models of the myocardium," *J. Mol. Cell. Cardiol.*, vol. 18, no. 7, pp. 661–678, Jul. 1986.

Appendix

List of Abbreviations

ADP	Adenosine Diphosphate
Akt	Protein Kinase B
APS	adapter protein with Plekstrin homology and Src Homology domain
ATP	Adenosine Triphosphate
BAT	Brown Adipose Tissue
BMI	Body Mass Index
CAD	Coronary artery disease
cAMP	Cyclic Adenosine Monophosphate
CAP	c-Cbl Associated Protein
CBL	proto-onco protein Cbl
CHF	Chronic heart failure
CrkII	CT10-related kinase
CT	Computed Tomography
$FADH_2$	Flavin Adenine Dinucleotide
FFA	Free Fatty Acids
GDP	Guanosine Diphosphate
GSK-3 β	Glycogen Synthase Kinase 3 β
GTT	Glucose tolerance test
IBAT	Interscapular Brown Adipose Tissue
IDCM	idiopathic dilated cardiomyopathy
IGT	impaired glucose tolerance
IR	Insulin Receptor

IRS	Insulin Receptor Substrates
IRS-1	Insulin Receptor Substrate 1
IRS-2	Insulin Receptor Substrate 2
NADH	Nicotinamide Adenine Dinucleotide
NE	Norepinephrine
P-Akt	Phosphorylated Protein Kinase B
PET	Positron Emission Tomography
PI3K	phosphatidylinositol 3-kinase
PKA	Protein Kinase A
RC	Respiratory Chain
SUV	standardized uptake value
SUV_{MAX}	Maximum Standardized Uptake Value
T1D	Type 1 Diabetes
T2D	Type 2 Diabetes
UCP-1	Uncoupling Protein-1
VMN	Ventromedial Hypothalamic Nucleus
WAT	White Adipose Tissue
2DG	2-deoxy-D-[H^3] glucose
^{18}F-FBnTP	4-18F-fluorobenzyltriphenyl phosphonium
^{18}F-FDG	2-deoxy-2-(18F)fluoro-D-glucose

Western Blotting Protocol

Western Blot

Day 1 - Gel Preparation and Running

What you need:
-gel apparatus with sponges (bench)
-glass plates (2 sized (1.5mm), 2 short plates) (bench)
-2 green plate holders (bench)
-combs same size as glass plates (bench)
-2x 50mL beakers (bench)
-1x 50mL tube
-10ml serological pipettes
-2 transfer pipettes
-Distilled water (DW)
-1.5M Tris pH 8.8 (4^{o}C)
-0.5M Tris pH 6.8 (4^{o}C)
-10% SDS (bench)
-40% acrylamide (4^{o}C)
-Ammonium persulfate (APS, 4^{o}C)
-TEMED (chemical storage cabinet)
-20% methanol (bench)
-0.1% SDS (bench)
-standard ladder (molecular marker) (-20^{o}C)
-gel running apparatus and container (bench)
-10ml syringe with needle

First remove samples from -80^{o}C to thaw on ice. If a white precipitate is present after thawing, place samples at 37^{o}C (using a heat block) until they are clear. This should only take a few minutes)

1. Obtain glass plates from drying rack on bench. If there is anything to clean off, use a kimwipe with DW
2. Place glass plates in green holders with the doors open, making sure both plates lay flush with the surface of the bench, and with each other. Next, while applying slight pressure to the tops of the glass plates, close the doors.
3. Place the well combs between the glass plates. Measure 11mm from the bottom of the well comb and place a mark. This is your pour line for your gel. Remove the combs and set aside.
4. Prepare 10% APS in a 1.5ml eppendorf tube: add 0.1g APS (kept at 4^{o}C) to 1ml DW. Triturate until dissolved. Make fresh daily.
5. Prepare your separating gel in a 50ml beaker with a stir bar. Your gel percentage depends on the weight of your target protein. Use the chart below to choose the appropriate percentage of gel to make.

Migration Pattern for Ready Gel Tris-HCl Gels

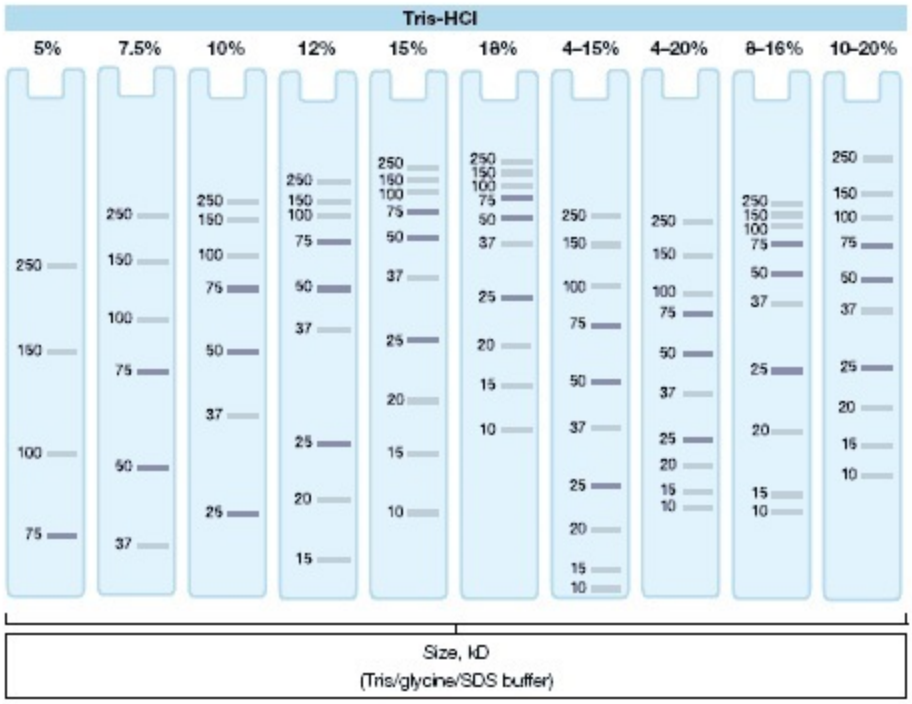

http://www.bio-rad.com/en-us/product/ready-gel-precast-gels/ready-gel-tris-hcl-precast-gels

Volume (ml)

Stock Component	**5%**	**7.5%**	**10%**	**12%**	**15%**
Distilled Water	12.3	10.93	9.68	8.68	7.18
1.5M Tris, pH 8.8	5	5	5	5	5
10% SDS	0.2	0.2	0.2	0.2	0.2
40% Acrylamide	2.5	3.75	5	6	7.5

The percentage of acrylamide determines the percentage of gel you are making. So, if you have 30% acrylamide to start, you will need to adjust volumes accordingly. For example, for a 10% gel, you will need 6.67ml of 30% acrylamide, and 8.01ml of DW. The DW is to make up the final volume of the solution to ~20ml.

6. Once the stock components are mixed for the appropriate separating gel percentage, place the glass plates that are in the green holders onto the sponges of the gel apparatus. Clip them in. Ensure they are sitting flush on the sponges.
7. ***See note below.** Place the beaker on a stir plate, mixing gently so as not to introduce bubbles. While mixing, quickly add 100ul 10% APS and 20ul TEMED. Allow to mix for 30 more seconds.

8. Using a transfer pipette, pipette gel mixture quickly between the plates, moving back and forth between the two sets of plates after each pipette-ful. Fill each set of plates to your marker line.
9. Carefully overlay the separating gel with 20% methanol using a syringe. Allow to polymerize for 30 mins. **Tip: leave your transfer pipette in your beaker containing left over gel solution. If this is polymerized after 30 minutes, your gel between the plates will be too.*
10. During this polymerization, mix your stock components for your stacking gel in a 50ml beaker containing a stir bar:

Volume (ml)

Stock Component	**4%**
Distilled Water	12.68
0.5M Tris, pH 6.8	5
10% SDS	0.2
40% Acrylamide	2

Note the use of a different Tris buffer

11. Once the gel is polymerized, pour the methanol down the sink and rinse the empty area between the plates three times with 0.1% SDS in a syringe (keep gels on the apparatus during this time). Ensure all SDS is emptied from this area by tilting the apparatus to the side and holding kimwipes to the top edge of the glass plates.
12. Place the beaker on a stir plate, mixing gently. While mixing, quickly add 100ul 10% APS and 20ul TEMED. Allow to mix for 30 more seconds.
13. Using a transfer pipette, overlay the separating gel with the stacking gel solution, filling to the top of the plates. Insert comb on an angle slowly so as not to introduce bubbles or displace too much gel solution. Allow to polymerize for 30 mins

***Note**: If a vacuum degasser system is available, make up both the separating and stacking gel solutions in their beakers with stir bars (without the APS and TEMED), mix briefly on the stir plate and place both beakers into the degasser. Put the lid on and turn the vacuum pump on. Leave for 20 minutes to remove the air from the solutions. After 20 minutes, turn the pump off, remove the separating gel, and while gently mixing on the stir plate, continue as for step 7. While the separating gel is polymerizing, put the lid back on the degasser to protect the stacking gel.

14. Put your molecular marker (ladder) on ice
15. Prepare your 1X Running Buffer as described in the Buffers section. This can be prepared in advance and stored at $4^{o}C$
16. Once the gel is polymerized, remove the combs by pulling them straight up and out. Remove the glass plates carefully from the holders and place them onto the middle section of the apparatus (containing the electrodes). The short plates of each set should be facing each other. Place this section into the beige middle part with clear “doors”. The doors should be open while the electrode is being inserted. Apply gentle downward pressure to the electrode section while closing the doors. Place this in the clear container.

17. Fill the middle section between the two gels with 1X Running buffer. Next, fill the clear container half way
18. Fill a Styrofoam box with ice. Create a spot to put the gel container. Place the gel container in this spot and push the ice against the sides of the container.
19. Begin loading your samples and ladder into the wells of the gel. You should load the wells of the gel closest to you first, and then turn the whole Styrofoam box to load the other gel.
    Typically, 5ul of ladder is loaded into the first well on your left. All wells should be filled to ensure the samples run straight down.
20. Once all samples are loaded, place the lid onto the container (black to black electrode, red to red electrode). Plug the cords into the power supply and turn on. Turn the voltage up to 200V and press the button that looks like a man running. Make sure to observe bubbles in the running buffer, signifying the gel is running.
21. The samples are condensed into a solid blue line while they run through the stacking gel. This ensures that all samples enter the separating gel at the same time, and therefore have the same amount of time to run through the gel.
22. Allow your gel to run until the blue dye front completely runs off the bottom of the gel. This typically takes just over 1 hour. While this is happening, gather your transfer supplies and make fresh 1X Transfer Buffer, as per the Buffers section. This can be made in advance and stored at $4^{o}C$.

Gel Transfer

What you need:
-transfer apparatus and container (bench)
-2x cassettes (bench)
-2 plastic containers for soaking filter paper, sponges, and membranes (bench)
-2 plastic containers for soaking the gels (bench)
-4x black sponges (bench)
-4x filter paper (bench)
-2x nitrocellulose membrane (bench)
-flat forceps (bench)
-1x transfer buffer ($4^{o}C$)
-ice pack ($-20^{o}C$)
-stir bar
-gel wedge

23. Once the gel is finished running, bring the entire container to the sink and dump out the running buffer. **Do not reuse this buffer.** Disassemble the apparatus to remove the glass plates.
24. Using the gel wedge, release the gel from the big plate so the gel is kept on the short plate. Cut the stacking gel off using the wedge and discard. Make a nick in the top left corner (usually the corner containing your ladder).

25. Add 1x Transfer buffer to a container. Place the short plate with the gel on it over the top of the container. By allowing the buffer to make contact with the gel, it should take the gel off of the plate itself. If this does not work, or if the gel stayed on the big plate rather than the short plate, use the wedge to gently lift the gel off of the plate and place into the buffer. Repeat with second gel in a separate plastic container.
26. Cut two membranes from the nitrocellulose roll using the filter paper as a size guide. Be careful not to touch the membrane with your gloves. Keep the blue paper on while cutting.
27. In another plastic container, place one sponge, one filter paper, one membrane, one filter paper, one sponge, and fill with 1X Transfer buffer. Repeat for second membrane.
28. Place all plastic containers on the belly dancer for 15 minutes, with slight agitation. This is necessary to equilibrate all components of the transfer "sandwich"
29. While these components are soaking, wash the running apparatus. To do this, re-assemble without the glass plates and fill the container with DW. Discard and repeat for a total of 3 times. Allow to dry on the drying rack or paper towel. **Do not hang.**
30. Assemble the sandwiches out of buffer on paper towel on the bench in the following order: clear side down, sponge, filter paper, membrane (move with forceps), gel (move with gel wedge, place so that cut corner remains on your left, ensure no bubbles), filter paper.
31. Use a 50ml tube to roll out any bubbles by starting in the middle of the filter paper and rolling outward. Repeat in opposite direction. Complete the sandwich by placing the second sponge onto the filter paper. Close the sandwich and repeat with the second one.
32. Place the sandwiches in the centre of the transfer apparatus with the black side of the cassettes facing the black side of the apparatus. Place the apparatus in the clear container (same one used for running of gel), add a stir bar, and place the ice pack in the unfilled space in the container.
33. Fill the container up to the edge with fresh 1X Transfer buffer
34. Move the apparatus to the clear door fridge onto the stir plate. Turn the stir plate on to low, making sure the stir bar moves easily. Place lid on top, red to red electrode and black to black electrode.
35. Turn the power supply on to 30V and run overnight.

Day 2 – Ponceau S, Blocking, and Primary Antibody

What you need:
-2x plastic containers (bench)
-flat forceps (bench)
-scalpel (bench)
-Ponceau S stain (bench, in the dark)
-0.1M NaOH (bench)
-1XTBST (bench)
-1 clear plastic sheet (bench)
-Blocking Solution
-primary antibody (storage conditions dependent on antibody)

-50ml conical tube

36. Press stop on the power supply, turn off the stir plate and return the apparatus to the bench.
37. On paper towel on the bench, open the sandwich (black side down) and cut the membrane to size using the scalpel, following the outline of the gel below it. If the transfer was successful, you will see the ladder on the membrane. Cut the nick in the corner again and flip the membrane over so that the nick is now on your left and place in a container. To keep track of which side is which, this nick should always be on your left, the side with your ladder. Repeat with the second sandwich.
38. Rinse the membranes with DW quickly then discard and add Ponceau S to the container (enough to cover the membrane). Place on belly dancer at low speed for 5 minutes.
39. During this staining, wash the transfer apparatus as you did the running apparatus. Allow to dry on the drying rack.
40. Discard the Ponceau stain down the sink and rinse the membranes with DW until all residual background red is gone, and only red bands remain. Scan this image on the computer.
    a. Open Canoscan
    b. Ethanol the scanner surface
    c. Lay membranes down on the surface, ensuring no bubbles
    d. Lay a clear plastic sheet over the membranes and close the scanner
    e. Select “Scan1”, source=platen, save to your file, click “ok”
    f. After the scan completes, the image is saved automatically. Check to make sure the picture is clear before destaining the membrane
    g. Ethanol the scanner surface again.
41. Destain the membranes by adding 0.1M NaOH to the container with agitation. It should destain within minutes.
42. Discard and rinse with DW, then wash the membrane for five minutes on the belly dancer at medium speed in 1XTBST (recipe in Buffers section, this can be made in advance and stored at room temperature)
43. During this wash step, prepare your blocking solution. Make sure to check the antibody information sheet of the antibody you will use to choose the appropriate blocking solution. Typically, 5% milk is sufficient, but BSA is also sometimes used. Skim milk is in a bag in the weigh room and BSA is kept at 4^{o}C. Make this fresh daily in 1XTBST. Typically, 25ml is used per membrane.
44. Once the wash step is complete, discard the 1XTBST and add blocking solution to the container. Place on the belly dancer at room temperature on a low speed for 1 hour.
    **Tip: If after you complete your western it comes out with nonspecific antibody binding, you can increase your blocking percentage to 8% to attempt to eliminate that.*
45. Just before the blocking step is complete, make up the primary antibody in a 50ml tube. The antibody information sheet should suggest a starting concentration for the antibody, as well as what to make it in. Typically, 5ml of antibody solution (5% milk or BSA made in 1XTBST) is made per membrane.

46. Once the blocking step is complete, if you are probing for multiple targets that run far enough apart on the gel, you can cut your membrane into two pieces and probe two at once. If you do this, you will cut using the scalpel, and use the smaller sectioned container. Each half of the gel should fit perfectly into the sections, allowing for the use of 2.5ml of antibody solution. If you do not cut the membrane, move the membrane to the smaller coloured containers that fit the whole membrane perfectly. This container requires 5ml of antibody solution. Place the container of choice on the rocker in the fridge (4^{o}C) at a low speed. Leave overnight.

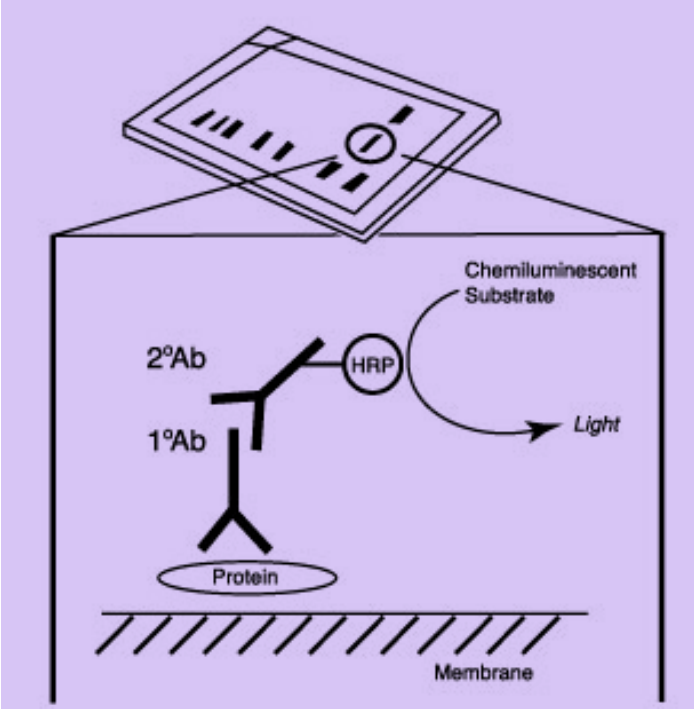

The information sheet that comes with your antibody has suggested blocking percentages as well as antibody concentrations. It also lists species reactivity, meaning which animal species they can detect. Ensure the antibody you choose is specific for the species of your sample. Some primary antibodies are specific to multiple animals. Your secondary antibody is made to target your primary antibody based on the animal that your primary antibody was made in. So, if your primary antibody is a goat anti-rat IL-6, it is detecting rat IL-6 in your sample, and was made in a goat. This means your secondary antibody must be anti-goat. Do not use a secondary antibody that is specific to your sample species. This will cause unspecific binding. So, if your sample comes from a rat, your secondary should not be anti-rat, and therefore your primary cannot be made in a rat.

Day 3 - Secondary antibody

What you need:
-2x plastic containers
-1XTBST (bench)
-Blocking solution (made fresh daily)
-secondary antibody (storage conditions dependent on antibody)
-15mL tubes (bench)

47. Remove membranes from the fridge and place in plastic containers. Add 1XTBST to cover and wash the membranes for a total time of 25 mins (medium speed on the belly dancer), changing the buffer every 5 minutes (discard down drain).
48. During the last wash, prepare the secondary antibody as per the antibody information sheet. Typically, 25ml of solution (usually in 5% milk made in 1XTBST) is used per membrane.
49. Following washes, discard the 1XTBST and add the secondary antibody solution. Place on belly dancer for 1 hour at room temperature at a low speed.
50. Discard the secondary antibody solution and perform wash steps as per step 47.
51. During the final wash steps, prepare your detection solution (If using enhanced chemiluminescence, continue as below) and set up the computer

Enhanced Chemiluminescence (ECL)

What you need:
-1XTBST (bench)
-1.0M Tris pH 8.5 (4^{o}C)
-DW
-30% H_2O_2 (4^{o}C)
-Coumeric acid - light sensitive (-20^{o}C)
-Luminol - light sensitive (-20^{o}C)
-1x clear plastic sheet (bench)
-2x 50mL tubes, one wrapped in tinfoil (bench, tinfoil in autoclave room)
-plastic wrap, taped flat to the bench
-kimwipes
-1ml pipette and tips
-flat forceps for membrane handling

*Take out coumeric acid and luminol, wrap in tinfoil and thaw on bench

Label two 50ml tubes as “Solution 1” and “Solution 2”. Add components listed below and keep solution 2 covered with tinfoil.

Solution 1		Solution 2	
Component	**Volume**	**Component**	**Volume**

Computer Set-Up

a. Turn on the ChemiDoc imager (2 things to turn on: black box beside the computer first, then big beige imager)
b. Open "Quantity One" on the computer, press "EPI White" on the imager
c. In the program, "File" > "ChemiDox XRS" > "Select" > "Custom" > "Western MWM"
d. Change the filter on the imager to the middle position (black stick on top)

52. After the final wash, discard the wash buffer. Using the flat forceps, move the membranes to the plastic wrap.
53. Pour ECL solutions together into one 50ml tube and mix by inverting. Pipette the mixed ECL directly onto the membranes, being sure to cover every part of it. Continue for one minute.
54. Dab excess ECL solution from membranes onto kimwipe by touching the corner of the membrane to the kimwipes, handling with the flat forceps. Place membranes onto clear plastic sheet and move to imager
55. Open drawer on imager to place membranes on sheet inside. In program, click "Live Focus" > "Freeze" (once it is in the appropriate position; it can be focused using the buttons on the imager) > "Auto Expose" > "Save". You now have an image of your ladder saved which is used to determine band size.
56. To detect your chemiluminescence, "File" > "ChemiDox XRS" > "Select" > "Custom" > "Sean Bryan Western", turn off the "Epi White" on the imager, change the filter to the first position (a O), click "Live Acquire", and fill in as 300 second exposure with photos taken every 60 seconds. Click "Save" and it will run. This time can be altered based on your target protein and how easily it can be imaged. You will have an idea of how well this timing is working after the first minute when the first picture pops up.
57. Once all images have been taken, the membrane can be discarded or stored at 4^{o}C in 1XTBS (1XTBST without the Tween 20) until a decision is made. The membrane can be stripped and re-probed for another target if necessary.

Buffers and Reagents

Tris 0.5M pH 6.8

Tris Base -12.1g
dH_2O - 200mL

Directions - Add Tris base to ~150mL of dH_2O, stir to dissolve completely. Adjust pH to 6.8 using concentrated HCl and adjust final volume to 200mL. Check pH and store in 4°C.

Tris 1.0M pH 8.5

Tris Base -24.23g

dH_2O - 200mL

Directions - Add Tris base to ~180mL of dH_2O, stir to dissolve completely. Adjust pH to 8.5 using concentrated HCl and adjust final volume to 200mL. Check pH and store in 4°C.

Tris 1.5M pH 8.8

Tris HCl-7.38g
Tris Base – 30.78g
dH_2O - 200mL
Adjust pH to 8.8 if necessary using concentrated HCl. Store in 4°C.

10% SDS

Sodium dodecylsulfate (SDS) - 10g
dH_2O - 100mL

4x Reducing Loading Buffer

0.5M Tris pH 6.8 - 10mL
dH_2O – 4.06mL
SDS – 2g
Bromophenol blue – 5mg
Glycerol - 10mL *add last!
-make 1ml aliquots and store at -20^{o}C. Before use, add 110ul **β**-mercaptoethanol to 1ml.

1x Running Buffer

Glycine – 14.4g
Tris Base - 3g
SDS – 1g
Make up to 1L with dH_2O

1x Transfer Buffer

Glycine – 2.93g
Tris Base – 5.82g
dH_2O – 700ml
70% Methanol - 200ml
Make up to 1L with dH_2O, store at 4^{o}C

10x TBS

Tris Base – 5.56g
Tris HCl – 24.24g
dH_2O – 800mL
-check pH, adjust with 12N HCl to pH 7.6

NaCl – 2.6g
Make up to 1L with dH_2O

1x TBST

dH_2O – 900mL
10xTBS – 100mL
Tween 20 – 1mL

Ponceau Stain

dH_2O - 475mL
Acetic acid - 25mL
Ponceau - 0.5g

*Note - light sensitive

Luminol

Luminol - 0.44g
DMSO - 10mL

Directions - Dissolve luminol in DMSO by vortexing. Pipette 420mL into eppendorf tubes and store in -20°C. *Note - light sensitive

Coumeric Acid

Para-coumeric acid - 0.15g
DMSO - 10mL
Directions - Dissolve coumeric acid in DMSO by vortexing. Pipette 100mL into eppendorf tubes and store in -20°C. *Note - light sensitive

FDG Dilution

1. Measure activity of received sample. If in a tube, transfer to a syringe.
   i. **For Large Volumes:** If activity is high enough that 1ml will contain enough activity (100+μCi) then add to eppendorf tube until the 1ml line is reached. Measure the activity.
   ii. **For Small Volumes:** Add full syringe to eppendorf tube and fill remaining amount with saline until the 1ml line is reached. Measure the activity.
2. Obtain concentration based on the activity measurement and volume (μCi/1ml).
3. Want final concentration of 200μCi/ml. Determine saline volume and FDG volume to acquire the desired concentration.

$$C_i\,(\mu Ci/ml)\,V_i\,(ml) \;=\; C_f\,(200\ \mu Ci/ml)\,V_f\,(1ml)$$

Ex:

$$3900\mu Ci/ml \times V_i = 200\mu Ci/ml \times 1ml$$

$$V_i = \frac{200\mu Ci}{3900\mu Ci/ml}$$

4. With a new syringe take up saline volume first (1000μl-V_i) and then the FDG volume (V_i).
5. Eject this into a new eppendorf tube and take up into the syringe again for injection.

6. Check actual activity (concentration) present and determine amount to inject 20μCi into the mouse. Should be 100μl. t

Dynamic Scan Images

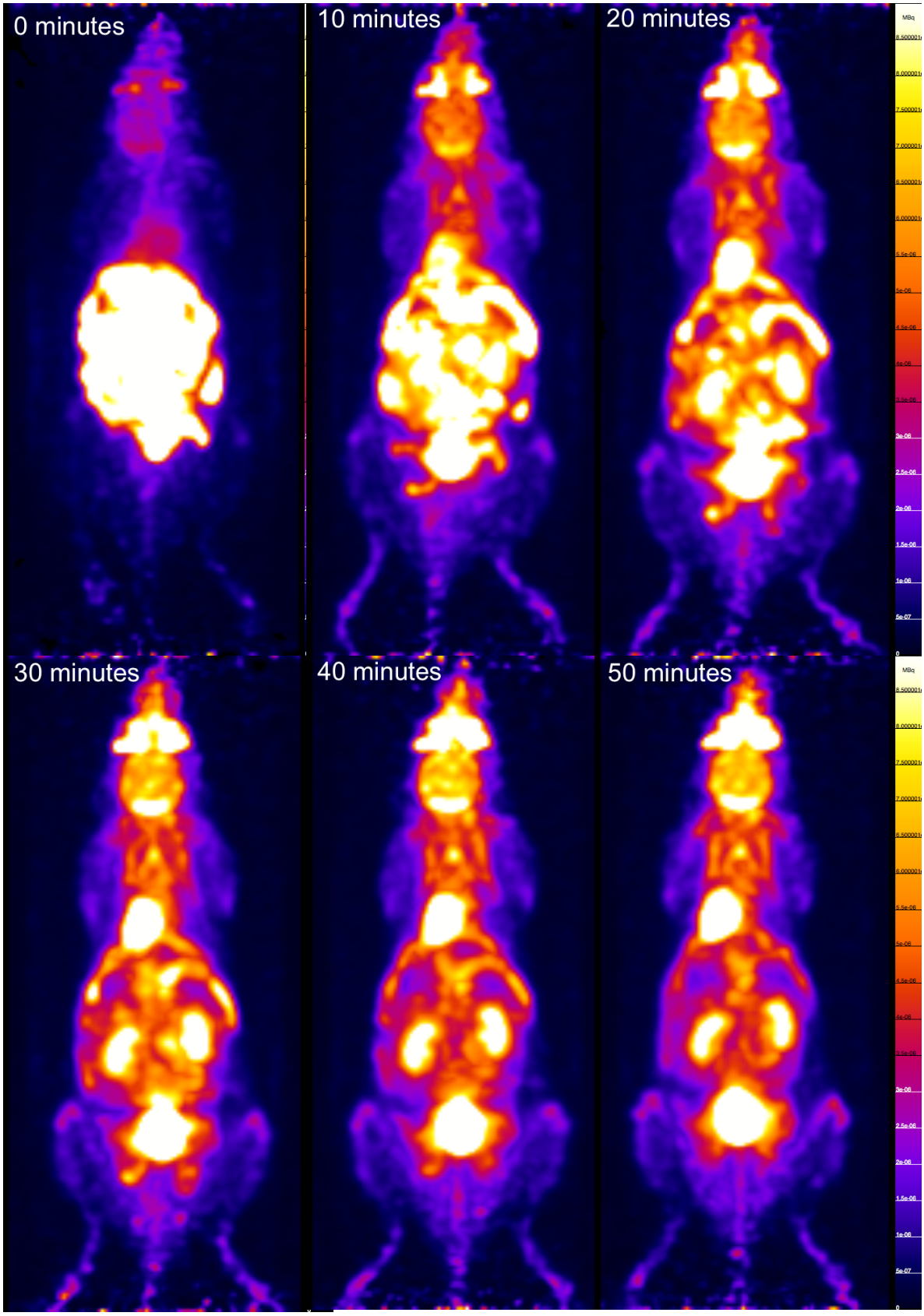

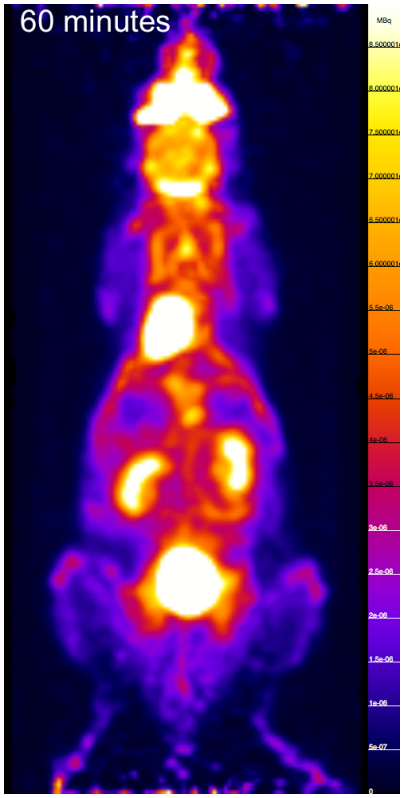

Results of preliminary 7x600 frame dynamic PET scan used to determine timing of static scanning. Scan completed immediately after injection of ~20μCi of ^{18}F-FDG through intraperitoneal injection. Anesthesia given for injection and throughout duration of scan, 2% isoflurane. Heated to 37°C for duration of scan. Time stamp in top left corner of image indicates time since injection of ^{18}F-FDG.